EFFECT OF SILVER DOPING ON THE OPTICAL AND PHOTOCATALYTIC PROPERTIES OF ZINC OXIDE THIN FILMS

A RESEARCH THESIS SUBMITTED IN FULFILMENT

OF THE REQUIREMENTS FOR THE DEGREE OF

MASTER OF SCIENCE IN CHEMISTRY

OF

THE UNIVERSITY OF NAMIBIA

BY

PATEMASELLA GAWANAS

201305044

APRIL 2020

MAIN SUPERVISOR: Dr. Likius Daniel *(Department of Chemistry and Biochemistry, University of Namibia)*

CO-SUPERVISOR(S): Prof. Veikko Uahengo *(Department of Chemistry and Biochemistry, University of Namibia*

Dedication

To my parents, Helga Namuandi and Erastus Namuandi

Declarations

I, Patemasella Gawanas, hereby declare that this study is my own work and is a true reflection of my research, and that this work, or any part thereof has not been submitted for a degree at any other institution.

……	……	……..
Name of Student	**Signature**	**Date**

List of Abbreviations and Acronyms

Abbreviation	Definition
Ag_2O	Silver (I) Oxide
AgO	Silver (II) Oxide
Ag-NPs	Silver Nanoparticles
Ag-NPs/ZnO	Silver Nanoparticles/Zinc Oxide composite
EtOH	Ethanol
H_4edta	Ethylenediaminetetraacetic acid
H_2O_2	Hydrogen Peroxide
IPCA	Index of Photocatalytic Activity
ITO	Indium Tin Oxide
LSPR	Localized Surface Plasmon Resonance
MB	Methylene Blue
MO	Methyl orange
MPM	Molecular Precursor Method
SPR	Surface Plasmon Resonance
UV/Vis	Ultraviolet/visible
XRD	X-ray Diffraction
$Zn(CH_3COO)_2 \cdot 2H_2O$	Zinc acetate dihydrate

List of Figures

List of Tables

List of schemes

Abstract

To study the optical and photocatalytic properties of zinc oxide (ZnO or zincite), thin films doped with metallic silver-nanoparticles (Ag-NPs), with various amounts of Ag (20 mol% ≤ n ≤ 80 mol%), were fabricated on a quartz glass substrate at 600°C in air using the molecular precursor method (MPM). The fabricated thin films were analysed and X-ray diffraction (XRD) patterns of Ag nanoparticles, zinc oxide, and composite AgNP/ZnO films were measured using an X-ray diffractometer. XRD patterns of ZnO thin film showed that the pure ZnO is c-axis (002) oriented. The XRD spectrum of pure Ag elucidated that the resultant silver film contains Ag crystallized in the cubic system. UV/Vis absorption spectra of the composite AgNPs/ZnO thin films revealed a surface plasmon resonance (SPR) peak around 410 nm. The 80% Ag film was found to experience the highest SPR. The intensity of wide-range absorption in the visible region increased with an increase in the Ag content in ZnO matrix, hence an increase in the SPR peak. This increase in the SPR absorption is due to the decrease in the amount of ZnO, hence the thin films become more metallic and also hence why the 80% film experiences the highest SPR. The bandgap of ZnO was also determined using the absorption spectra of naked ZnO and composite AgNPs/ZnO thin films and was found to significantly decrease from 3.30 eV for a naked ZnO to 2.30 eV for the composites. The photocatalytic activity of MO decoloration was investigated quantitatively by monitoring the changes between the initial MO absorption spectra and the final MO absorption spectra intensity positions, as well as qualitatively by determining the decoloration rate of MO (nM min^{-1}). The absorption spectra of decoloration of 0.02×10^{-3} M MO aqueous solution tested under visible light irradiation and dark, for 8 h respectively, by employing the naked ZnO thin film, pure Ag-NP, composite thin films and the blank. The decoloration rates monitored by the

absorption intensity of the MO solution indicated that the composite thin films of Ag are effective under visible irradiation. The index of photocatalytic activity (IPCA) values extracted from decoloration rate of 0.02×10^{-3} M MO solution by photoreaction with each thin film and a blank show that, under visible light irradiation, none of the composite samples exhibits more photoactivity than the 80 % Ag composite thin film. All of the composite samples are more photoactive than pure ZnO under both dark and visible light irradiation. The different results reveal that the photoactive enhancement mechanisms under dark and visible light irradiation are different. Undoped ZnO exhibits no photocatalytic reaction properties. Absorption spectra of the thin films, suggested that the visible responsive activity of the composite thin films is due to SPR of AgNPs. It was also elucidated that the vis-responsive level of the composite thin films corresponds to their change in band gaps depend on the Ag content. On the basis of photo excited electron transfer from AgNPs to the ZnO conduction band, the excellent response to vis-light and major factors affecting the photo response were clarified by SPR

Table of Contents

Acknowledgements

The three years that it took to complete this Masters was a journey that seemed never ending and it certainly was not an easy one that could not have been a reality without the following individuals. I am highly appreciative to **Dr. L. S. Daniel** for his guidance and constant supervision and the constant drive to complete this thesis. His never-ending assistance and willingness in helping to finalise this thesis will forever be remembered. The Chemistry/Biochemistry Department is also recognized for proving their laboratory the necessary lab work and resources to carry out this, now successfully completed research. A great thank you to my co-supervisor, **Prof. V. Uahengo**, for making certain that the required research equipment and chemicals were available and for availing time in his busy schedule to co-supervise my work.

I would sincerely like to thank my incredible team members **Paulina Endjala**, **Rocha Kaffer**, **Moses Joseph**, **Magano Kalipi, Johannes Naimhwaka, Theodor N. N Nghilalulwa** and **Mrs. Theopolina Amakali** for the great assistance in the laboratory work and sharing of useful knowledge.

Lastly, I would like to thank the most important people in my life, my family. Thank you, **Mother Helga Namuandi**, for raising a strong, hardworking woman that is able to conquer anything she puts her mind to, and my **Father Erastus Namuandi**, for being a constant source of strength and raising an independent woman. I am forever indebted to you both.

Chapter 1: Introduction

1.1 Background of the study

Photocatalysis is one of the main chemical routes for destruction of environmental toxic pollutants. Metal oxide semiconductor heterogeneous photocatalysts are playing an important role in many industrial and technological processes, in both environmental and biomedical application [1]. Among many metal oxides, zinc oxide (ZnO) possesses excellent photocatalysis properties [2]. Three dissimilar optical band gap values (3.1, 3.2, and 3.3 eV) of ZnO single crystals at room temperature have been reported in literature [3]. It is however concluded that the band gap of ZnO crystals at room temperature is 3.3 eV and this was established by comparing the optical properties of ZnO crystals by using a variety of optical techniques [3]. Truong et al. [4] found that when ZnO catalysts are subjected to sunlight irradiation with photons of energy equal or higher than their band gap (3.3 eV), the generated electron hole pairs can induce formation of reactive oxygen species (ROS), such as •OH and O_2, that are directly involved in the oxidation processes leading to degradation of natural organic matters (NOM) such as methyl orange (MO) [5].

Nanosized noble metal particles or nanoparticles have received widespread attention owing to their vital potential applications [6]. Recent research extensively describes and reviews the properties, preparation methods and applications of nanoparticle catalysts [7]. Many researchers [8 - 10] have demonstrated that the addition of noble metals, such as Pt, Au, Cu, Ag, and metal oxide semiconductors to ZnO, can effectively enhance the degradation efficiency of photocatalytic reactions. This is because they act as an electron trap promoting interfacial charge transfer processes in the composite systems. As a result, more photo induced holes will have opportunity

to participate in the oxidation reactions on the surface. Nevertheless, the chance of recombination of photo induced electrons and holes will increase leading to reduction in the rate of a decomposition reaction with further loadings of noble metal particles [11].

There are many techniques for the fabrication of nano porous ZnO films such as pulsed laser deposition [12], thermal evaporation [13], magnetron sputtering [14], electrodeposition [15], sol-gel [16], spray pyrolysis [17] and molecular precursor method (MPM) [18]. Among these methods, MPM has received increasing attention due to the easy control of film morphology, low-cost processing, high throughput, and the possibility to use various substrates. Unfortunately, ZnO has many drawbacks which limits its practical applications in the field of photocatalysis. One of the drawbacks is that the band gap of ZnO is located in the UV region ($\lambda < 400$ nm), which represents less than 5% of the entire solar spectrum. Similarly, ZnO has a high electron/hole recombination rate, which effects the efficiency of dye degradation [4]. Additionally, the light etching effects make ZnO unstable [19]. Therefore, there is a tendency of adding an amount of plasmonic metal over the ZnO surface to overcome these drawbacks. Many metals such as platinum (Pt), silver (Ag), copper (Cu), aluminium (Al), and palladium (Pd) can act as plasmonic metals. The absorption of ultraviolet–visible (UV–Vis) light of ZnO can be enhanced by the addition of noble metal nanoparticles which exhibit surface plasmon resonance [20]. Plasmonic nanoparticles exhibit absorption cross sections which can be several or even tens of times higher than the physical cross section [21]. The plasmonic nanostructures are widely used in many applications due to their unique optical properties due to the existence of surface plasmon resonances. The surface plasmon resonance (SPR) is generated when the free electrons within the nanoparticles are induced to oscillate coherently by interacting electromagnetic fields of the

incident light. The surface plasmon resonance causes strong localized electric fields around the nanoparticles which improve the interaction between light and nanostructures [22]. The oscillating conduction electrons collide with the ion lattice of the plasmonic nanoparticles due to the light-induced electric field. These electron-ion scattering events are translated into generated heat. Plasmon-induced hot-electron generation at the metal/semiconductor interface improves the efficiency and durability of photocatalysts [23]. However, most of these metals (Cu, Pd, and Al) are susceptible to oxidation which causes a negative effect on the plasmonic resonance [23]. This leaves Pt and Ag as excellent co-catalysts for photocatalytic H_2 production due to its high chemical stability and non-toxicity as compared with other noble metals. However, Pt is very expensive compare to Ag, consequently the latter is extensively studied [23, 24.].

Moreover, the SPR absorption band (410 nm) of Ag is very close to the band gap (3.3 eV) of ZnO, which increases the energy transfer between Ag and ZnO due to the strong local electrical field induced by SPR. Also, the work function of the metal determines the electron transfer direction for the metal/ZnO nanostructures. Ag has a higher work function than ZnO, which is why Ag is one of the best choices [25]. By spin coating the composite precursor solution on quartz glass substrates, the potential of producing metallic Ag−nanoparticles/zinc oxide (Ag NP/ZnO) composite thin films with various and unprecedentedly high Ag particles, up to 80 mol % of Ag homogeneously distributed in a ZnO matrix may fabricated using MPM. This is because

MPM offers excellent miscibility of the silver and titania precursor solutions, it is also effective for overcoming the limitations in miscibility of the conventional sol–gel method. This method is necessary for fabricating Ag/ZnO composite thin films with amounts of Ag ≤ 80 mol% [26].

Methyl orange (MO) is a heterocyclic aromatic chemical compound with molecular formula $C_{14}H_{14}N_3NaO_3S$. It has many uses in a range of different fields, such as biology and chemistry. It appears as a solid, odourless, dark-orange powder that yields an orange solution when dissolved in water at room temperature. This dye is stable and incompatible with bases, reducing agents, and strong oxidizing agents. During a chemical or biological reaction pathway, this dye compound not only depletes the dissolved oxygen in water bodies but also releases some toxic compounds to endanger aquatic life [27]. It has been reported that MO is capable of being photobleached, demethylated, and photodegraded under visible light irradiation on a suitable catalyst [26]. Sangpour et al. [27] add that "Some of the nanosystems such as ZnO film or its nanoparticle catalysts can decompose MO to safe solution under UV irradiation" (pg. 13955).

This is the first comprehensive and comparative research on the fabrication, characterization, and study the photocatalytic activity on the Ag-NP/ZnO composite thin films with various and high composition of Ag particles (up to 80 mol% of Ag homogeneously distributed in a ZnO matrix) fabricated using molecular precursor method (MPM) for the degradation of MO. According to Nagai et al. [28], 'MPM is based on the design of metal complexes in coating solutions with excellent stability, homogeneity, miscibility, coatability, etc., which have many practical advantages' (p.300). It eliminates organic ligands in the precursor metal complexes and provides

important functions to the metal oxides in the chemical fabrication of Ag/TiO_2 composite thin films with high conductivity [28]. Therefore, using MPM would be possible in fabricating homogeneous metal oxide such as ZnO thin films on substrates using heat treatment methods. In this thesis, the fabrication and effect of addition of silver nanoparticles into ZnO-based system matrices is compared to pure ZnO films during the photocatalytic degradation reaction of MO in the presence of sunlight irradiation.

1.2 Statement of the problem

Current methods used to fabricate thin films are complicated and they produce inhomogeneous thin films especially at high doping concentrations. Moreover, the information on the suitability and efficacy of this technique as a viable alternative to producing quality ZnO thin films as photocatalysts have not been established. Therefore, the MPM is used to fabricate ZnO thin films, additionally, this method of preparation and characterization of new fabricated ZnO would contribute towards the knowledge of the fabrication and the rate enhancements of decolourization of organic compounds. ZnO can be used as solar material due to decreased bandgap. This will prove the hypothesis that the metallic plasmonic in a semiconductor enhances rates of photocatalytic reactions currently reported in literature.

1.3 Objectives of the study

The objectives of the study were:

(i) To fabricate pure ZnO and Ag-NP/ZnO composite thin films using MPM.

(ii) To determine the structural and optical properties of the fabricated thin films.

(iii) To investigate the photocatalytic reduction of Methyl orange by Ag-NP/ZnO composite thin films.

1.4 Significance of the study

The fabrication and characterisation of Ag-NP/ZnO composite thin films were investigated for the first time using a simpler method. Introduction of silver led to a red shift in the optical band gap of zinc oxide. Economic value of ZnO will be enhanced. The findings validated a positive relationship exists between Ag-NP surface plasmon absorption and the rate enhancements of decolourization, thus proving the hypothesis that the metallic plasmonic in a semiconductor enhances rates of photocatalytic reactions.

Chapter 2: Literature review

2.1 Importance of composite materials

Composites are made by combining one or more substances or materials with different physical and chemical properties. The positive aspects of composite materials range from high durability, corrosion resistance, low cost, light weight to tight tolerance. The selection of suitable combinations of matrix and strengthening material can lead to a new material that meets the requirements of a particular application [29]. Recent research showed that the distinct components of the composite materials remain separate within the finished structure [30]. The first use of composite materials dates back to as far as 1500 BC. when a mixture of mud and straw were used to create strong and durable buildings [31]. Due to the advantages and the presence of a combination of properties in composite materials, it has led to the widespread application in many different industries [31]. The industries that greatly employ the use of composite materials are construction industries, aerospace and car industries. There also exist composites that are on the nano scale related greatly to this research termed nanocomposites. Nanocomposites are generally defined as a matrix to which nanoparticles are added to advance a particular property of the material [32]. Various applications of nanocomposites include producing batteries with greater power output, speeding up the healing process for broken bones, producing structural components with a high strength-to-weight ratio, lightweight sensors and nanoparticles composite thin films.

Daniel and his team [33] use the MPM to dope silver nanoparticles in to the titanium oxide matrix fabricated with heat-treatment of the mixed precursor films at 600°C in air. As a result, Ag-NP/TiO_2 composite thin films containing various concentrations (10-80 molar %) of the silver nanoparticles were tested as potential photocatalysts. The photocatalytic activity of these composite thin films was compared to the photocatalytic activity of pure TiO_2 in the photo oxidation reaction of model compound, methylene blue (MB). It was proven that a large amount of silver nanoparticles (>10% Ag molar concentration) greatly decrease photocatalytic activity of TiO_2 under UV light irradiation. The Ag-NP/TiO_2 composite thin films showed oxidation activity significantly higher than pure TiO_2 under visible light irradiation.

2.2 Fundamental aspects of mixed metal oxide nanoparticles

Due to the essential properties and value in applications of metal oxide composites, noteworthy efforts have been devoted into the growth of oxides as composite and as thin films [30]. Moreover, oxide-based compounds indicate a diverse assortment of properties [30]. Akram et al. [34] stress that "Mixed Metal Oxides (MMO) have been attracting growing attention because these nanoparticles have wonderful energy storage applications" (p.18). Various synthesis methods of MMO's have been developed by scientists as outlined and explained briefly below as different synthesis methods for the preparation of ZnO thin films.

2.3 Fabrication of silver doped ZnO thin films

Doped ZnO thin films are very interesting for the production of optical devices [28]. There a various method of fabricating ZnO thin films namely molecular beam epitaxy [35], metal organic vapor deposition [36], sputtering [37], MPM and sol-gel spin coating [38]; chemical vapour deposition, sputtering and radio frequency sputtering have been employed in the synthesis of ZnO thin films [39]. The MPM is based on the design of metal complexes in coating solutions with excellent stability, homogeneity, miscibility, coatability, etc., which is a practical advantage compared to other methods [28]. Razeen et al. [39], however, explain that 'among these methods, sol-gel spin coating has some advantages such as chemicals control, doping feasibility, and low-cost fabrication' (p.131). The precursor films involving metal complexes should be amorphous, just as with the metal/organic polymers in the sol–gel processes; if not, it is impossible to obtain metal oxide thin films spread homogeneously on substrates by subsequent heat-treatment [31].

2.3.1 Molecular Beam Epitaxy

Research outlines that Molecular Beam Epitaxy (MOE) is an advanced ultra-high-vacuum facility to make compound semiconductor materials with great precision and purity [40]. MOE is a prevailing technique both for research into new materials, layer structures, and for producing high-performance semiconductor devices [40]. Pan et al. reveal the resultant structure of ZnO grown on sapphire substrates by plasma-assisted molecular beam epitaxy [41] and the structure is shown in Figure 1 below.

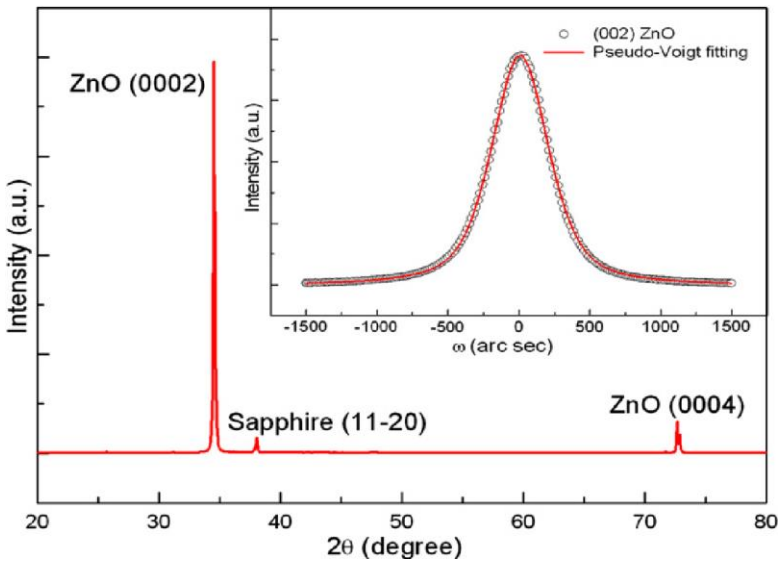

Figure 1: XRD spectrum of ZnO thin film grown on a-plane sapphire (41: pg. 4432)

They established that ZnO thin films could be effectively grown on a-plane sapphire using MBE, which display good crystalline and optical properties [41].

2.3.2 Metal organic vapor deposition

Metal Organic Chemical Vapour Deposition (MOCVD), sometimes called Metal Organic Vapour Phase Epitaxy (MOVPE) is a much higher throughput technique when compared with MOE [42]. MOCVD is dependent on the gas phase transfer of the material to be deposited on the substrate; the deposition occurs via a chemical reaction at the substrate surface and results in a high quality epitaxial thin-film deposition [42]. Zeng et al. fabricated boron-doped zinc oxide thin films grown by metal organic chemical vapor deposition with various boron contents and under different

deposition temperatures [43]. The XRD patterns of the resultant thin films are displayed below in Figure 2.

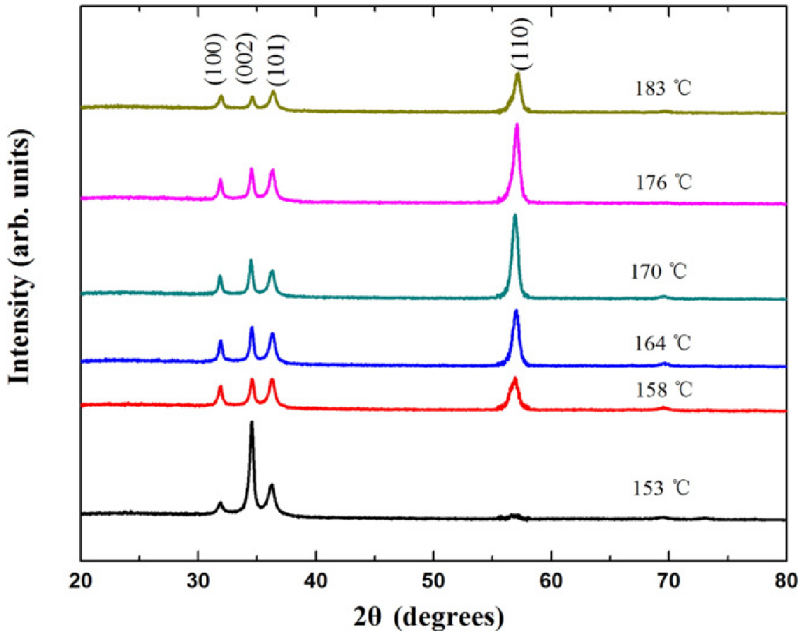

Figure 2: XRD patterns of BZO films deposited at different substrate temperature (43: pg. 260)

2.3.3 Sputtering

Sputtering is a method that uses inflated temperatures at high vacuum to eject atoms or molecules off a material surface [44]. In this technique, the target material and the substrate are positioned in a vacuum chamber and a voltage is applied between such that the target is the cathode and the substrate is attached to the anode [44]. A plasma is produced by ionizing a sputtering gas (inert gas) which bombards the target and sputters off the material to be deposited [44]. The most prominent advantage of this technique is its ability to coat large areas uniformly. Figure 3 below demonstrates the sputtering technique.

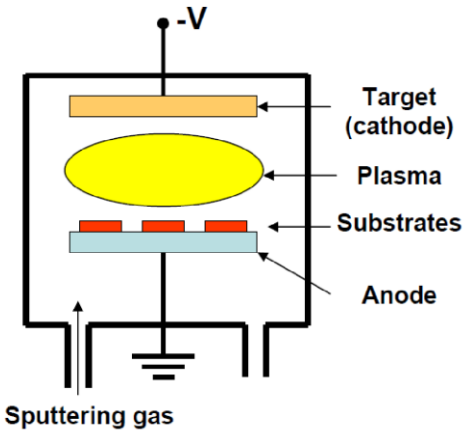

Figure 3: Illustration of sputtering (44: pg.1)

2.3.4 Sol-gel spin coating

Sol-gel is a procedure whereby solid materials are formed from small molecules. According to Pathak et al. [45] sol–gel-based coatings are being utilized in each sector of engineering application, however, the industrialization of sol–gel coatings is still in the initial stages of development. Khan et al. [46] fabricated highly oriented and transparent undoped ZnO thin films on ultrasonically cleaned quartz substrates by the sol-gel technique and the films were prepared on ultrasonically cleaned quartz substrates using a spin-coating unit. The XRD pattern of the films fabricated using this technique [46] yielded "peaks that correspond to the peaks of standard ZnO" (pg. 341). The XRD pattern of ZnO thin films fabricated using sol-gel method is shown in Figure 4 below.

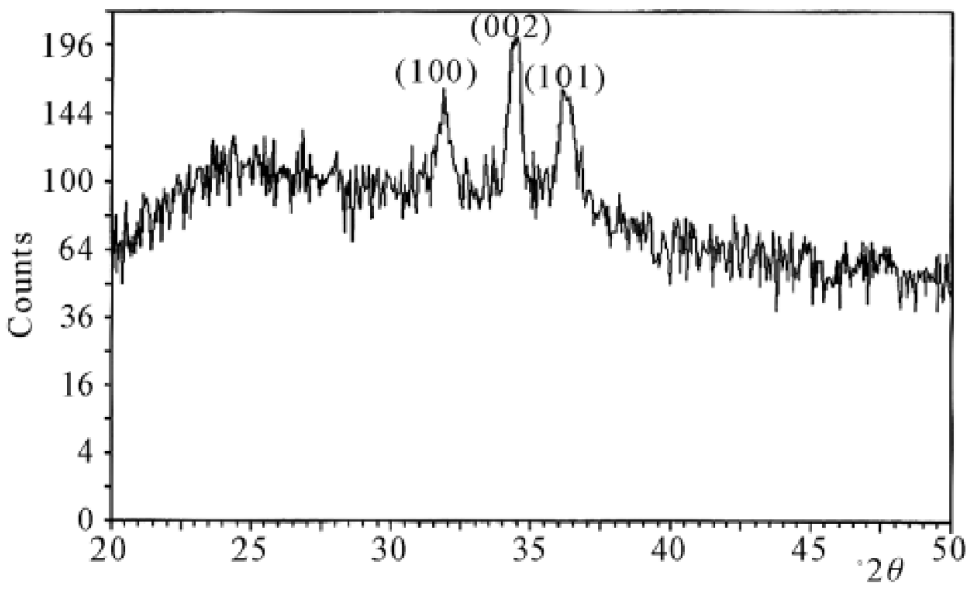

Figure 4: XRD pattern of ZnO thin films fabricated using sol-gel method (46: pg.341)

The XRD pattern of ZnO thin films fabricated using sol-gel method is shown in Figure 4 above.

Further research [47] shows that ZnO thin films doped with manganese were successfully fabricated by the sol-gel method. The manganese content was varied from 0 to 7% of molar weight [47] and XRD was used to study the microstructure of the fabricated films "reveal that all the films are single crystalline with a hexagonal wurtzite structure" (pg. 53); Figure 5 shows this.

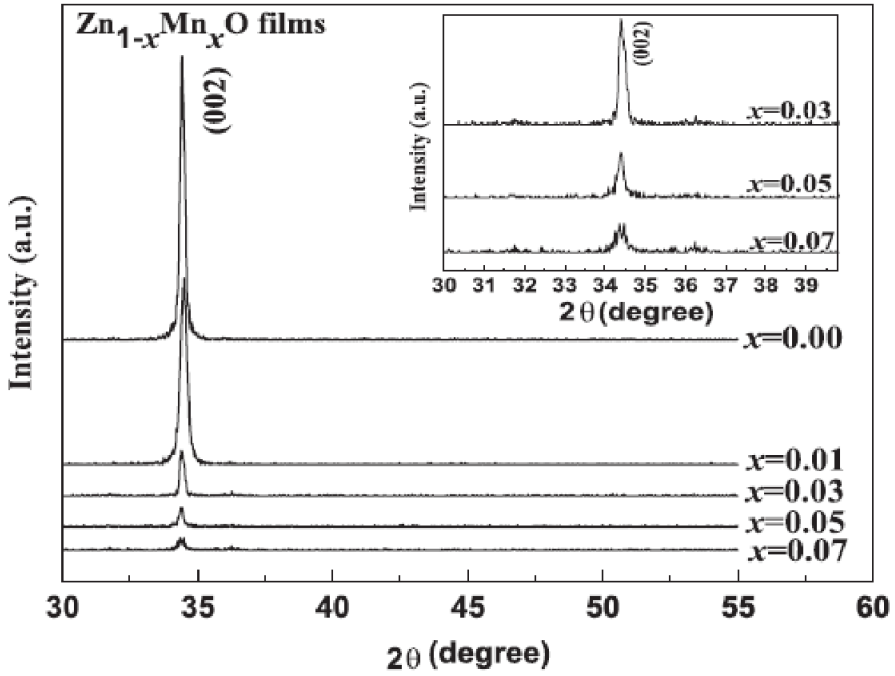

Figure 5: XRD pattern of Mn-doped ZnO thin films (47: pg.53)

2.3.5 Molecular Precursor Method (MPM)

MPM is a wet process for the formation of thin films of various metal oxides [29]. Nagai et al. [29] clarify that "Metal complex anions with high stab5ility can be dissolved in volatile solvents by combining them with the appropriate alkylamines; the resultant solutions can form excellent precursor films through various coating procedures" (pg. 300). The concept of the technique is to apply an alcoholic precursor solution of an EDTA metal complex on the substrate and heat treat the metal at temperatures of 500-700°C. Heat treatment is necessary to eliminate organic ligands from metal complexes involved in spin-coated precursor films and to fabricate thin films of crystallized metal oxides or phosphates. According to Nagai et al. [29], the resultant crystal size of the oxide particles produced by the MPM was found to be smaller compared to those synthesized by the sol-gel method. The crystallites size generated from this method of fabrication is attributed to the nucleation process of crystallized metal oxides. In a typical metal nanoparticle/composite

material synthesis, it is ideal that the crystallite size of metal particles be smaller than that of the dopant metal oxide. Another group of researchers [33] fabricated TiO_2 thin films and composite Ag-NP/TiO_2 films using the MPM and the XRD analysis (shown in Figure 6 below) revealed that "no phases other than titania and metallic silver were present in the composite thin films" (pg. 3893), which is further evidence that the MPM is an excellent method.

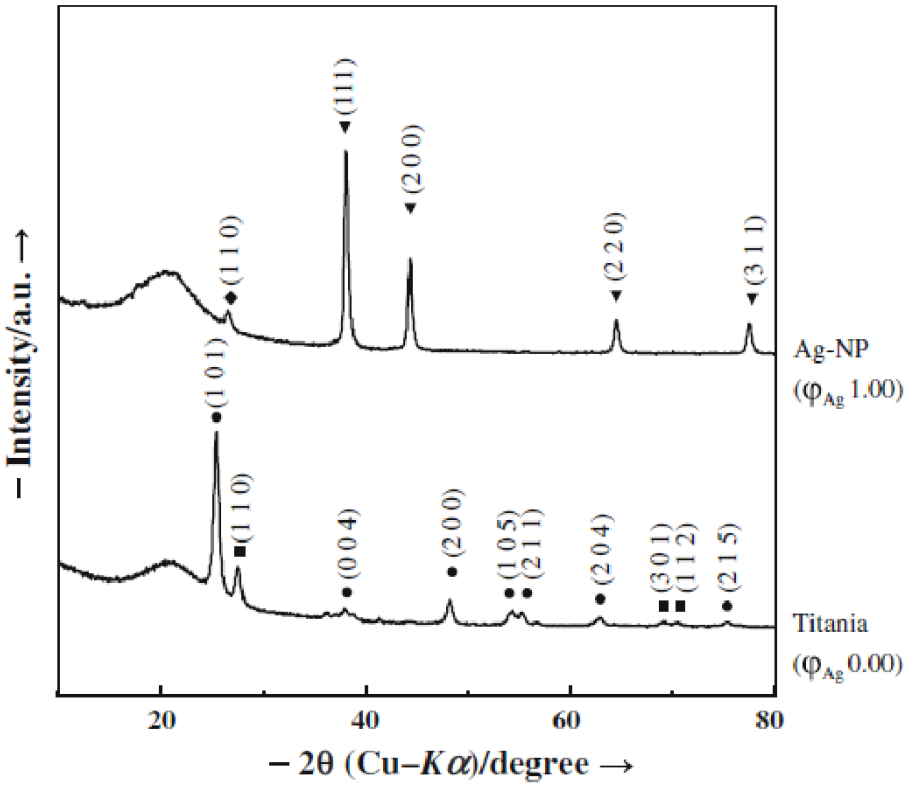

Figure 6: XRD pattern of TiO_2 and AgNPs/TiO_2 thin films fabricated using the MPM (33: pg. 3893).

2.4 Modification of ZnO to be active under visible light

Candal et al. [48] mention that semiconductors such as ZnO, ZnS, Nb_2O_5, Ta_2O_5, and $BiTaO_4$ have been described to exhibit excellent performance as photocatalysts. Semiconductors doped with a

transition metal as photocatalysts have been employed in order to improve their physical properties. There are semiconductors with narrow band gaps such as, Fe_2O_3 and CdS, with band-gap values of 2.5 and 2.3 eV, respectively. They however do not exhibit catalytic properties as the energy levels of either their conduction or valence bands are unsuitable to construct light-harvesting assemblies [31]. Various techniques have been tested to enable ZnO to be active under visible light and these techniques include surface modification via organic materials, semiconductor coupling, band gap modification by creating oxygen vacancies and oxygen sub-stoichiometry and co-doping of non-metals [49].

2.4.1 Surface modification via organic materials

Photocatalytic oxidation of several harmful inorganic pollutants (arsenic, lead, air pollutants, etc.) and organic dyes in industrial wastewater has been carried over TiO_2 and ZnO semiconductor oxides under UV light irradiation [49]. Li et al. [50] explain that the pre-requisite for an efficient photocatalyst is that the redox potential for the release of hydrogen and oxygen from water and for the formation of active species like hydroxyl radicals (OH•), hydrogen peroxide (H_2O_2) and super oxide ($O_2^{\bullet -}$) must lie within the band gap of a semiconductor photocatalyst, Figure 7 below illustrates this. Narrow band gap semiconductors that are able to absorb visible light are generally unstable in aqueous suspensions and consequently are not suitable for photocatalytic applications [51]. ZnO being a wide bandgap semiconductor is suitable for degradation of organic pollutants due to its high quantum efficiency [51], however it is only active under UV light irradiation. Research conducted by Rehman et al. [49] suggest that "dye sensitization is one useful tool to induce visible light photocatalysis on the surface of wide band gap semiconductors like TiO_2 which are otherwise inactive under visible light" (pg. 561).

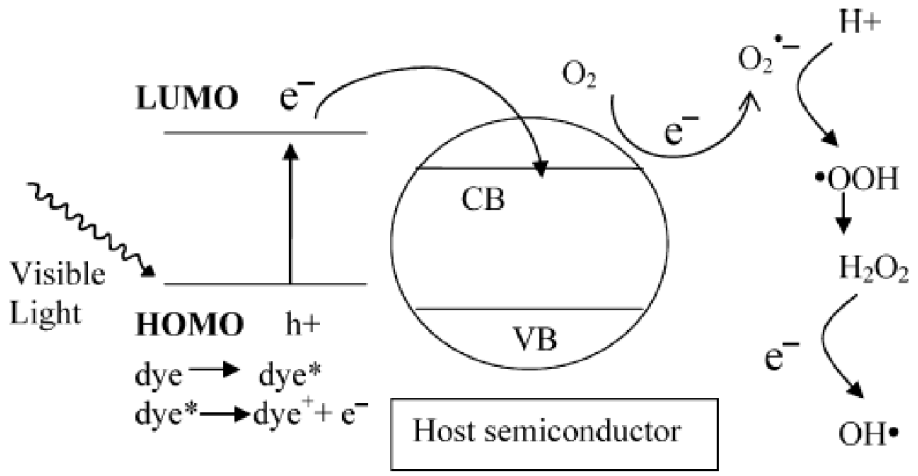

Figure 7: Visible light activation of a wide band gap semiconductor by dye sensitization (49: pg. 561)

2.4.1 Band gap modification by creating oxygen vacancies

Visible light absorption of ZnO materials is achievable by introducing oxygen vacancies. The oxygen vacancy method is a self-doping tool that allows no introduction of any impurity elements, which is more favourable on conserving the inherent crystal structures of ZnO and in turn leads to improved photocatalytic performances under visible light irradiation. However, there are challenges in the synthesis of oxygen vacancy in rich ZnO samples. Wang et al. [52] explain that "The oxygen vacancies in ZnO are unstable after high temperature annealing treatment, which would gradually transform from yellow to white again when it is cooled down to room temperature" (pg. 4024). The group of researchers continue to add that the concentrations of oxygen vacancies tend to be low and this leads to inadequacy when attempting to expand the visible light absorption [52]. Experimental results have successfully indicated that the presence of oxygen vacancies in ZnO can effectively expand the visible light absorption range of ZnO as well as effectively enhance their visible light photocatalytic efficiencies [52]. It has also been

established that higher oxygen vacancy concentrations would lead to stronger visible light absorption [53]. Figure 8 displays the UV–Visible diffuse reflectance spectra and the energy band gap of the prepared ZnO and ZnO_2 samples. A Structure model of oxygen vacancy in a ZnO cell model is shown in Figure 9 below.

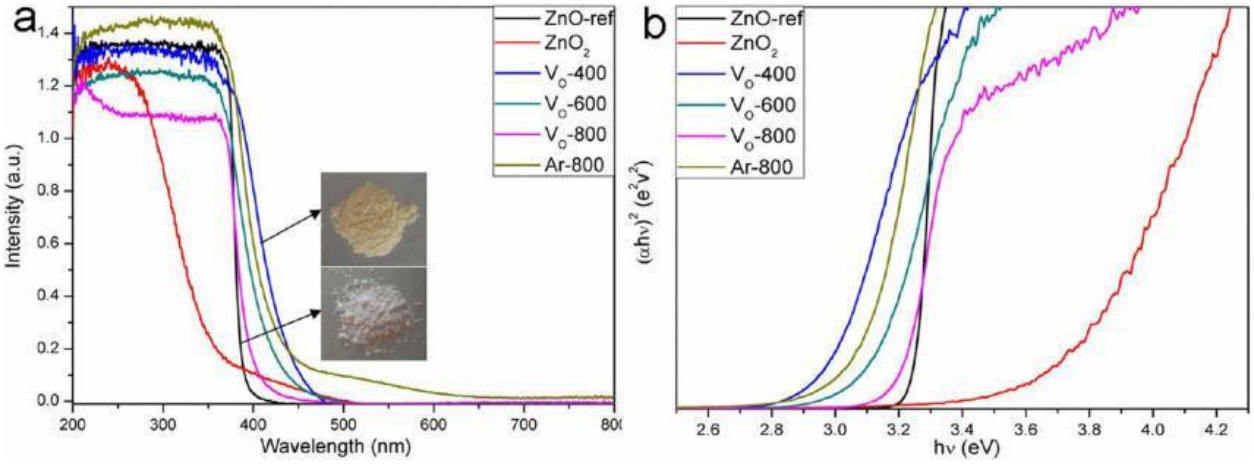

Figure 8: UV–Visible diffuse reflectance spectra (a) and the energy band gap (b) of the as–prepared ZnO and ZnO_2 samples (52: pg. 4027)

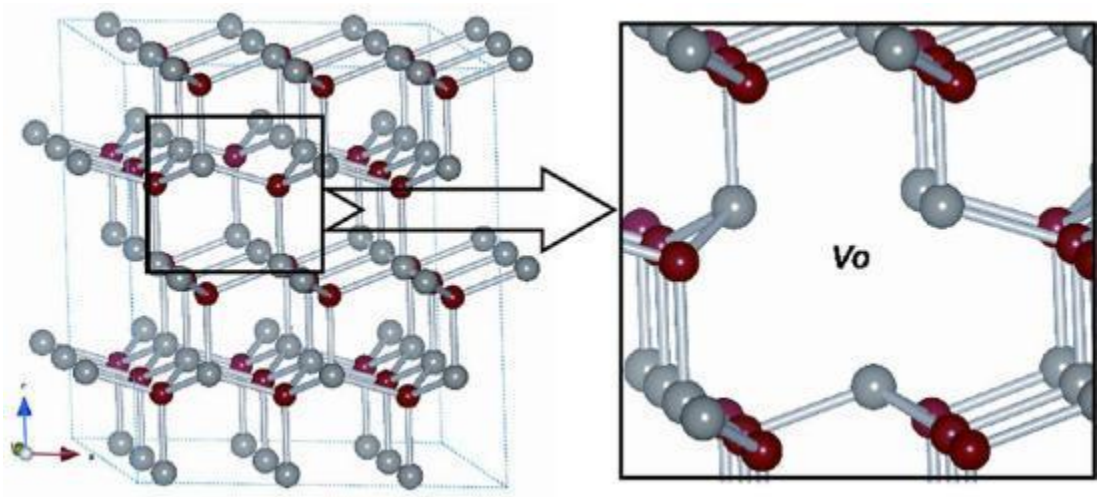

Figure 9: Structure model of oxygen vacancy in a 3*3*2 super cell; the balls in grey and red represent Zn and O atoms, respectively (52: pg. 4029)

2.5 Characterization of the structural properties of Ag-NP/ZnO thin films

XRD is based on the diffraction of an X-ray incident beam by reticular planes of crystalline phases in a thin film sample [30]. Likius [30] adds that "The beam is diffracted at specific angular positions with respect to the incident beam depending on the phases of the sample" (pg.101). Research conducted by Khan et al. [46] reveal that the (100), (101) and (002) diffraction peaks of ZnO can be observed in the XRD pattern, showing the growth of ZnO crystallites along different directions as shown in the Figure 10 below.

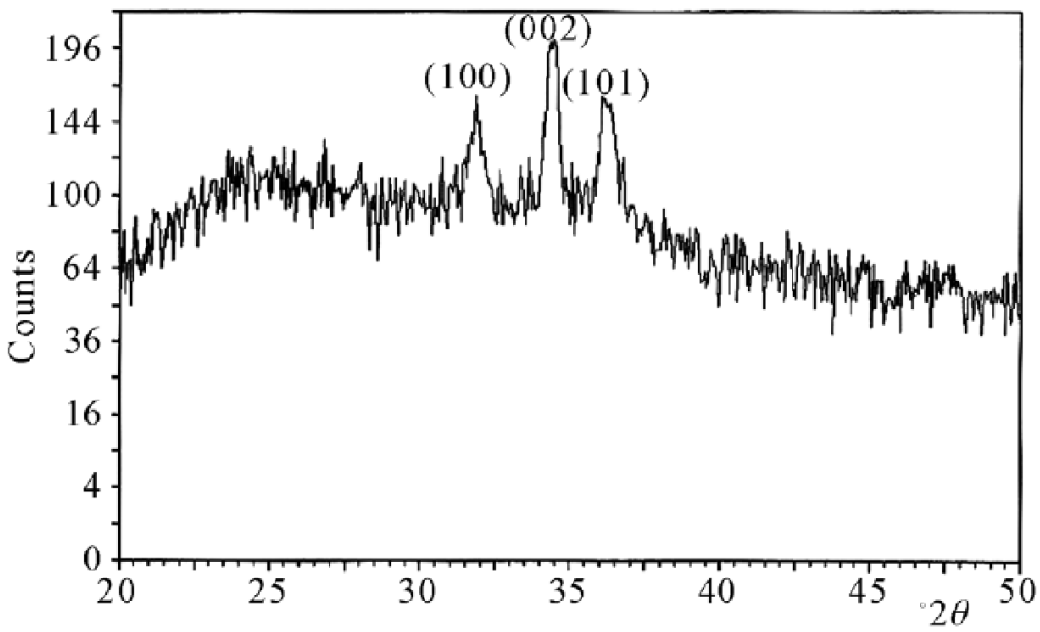

Figure 10: XRD pattern of ZnO thin films (46: pg.341)

A typical XRD spectrum consists of a plot of reflected intensities versus the detector angle 2θ, an example of an XRD pattern of ZnO thin films is shown above in Figure 10. The analysis data

obtained is typically compared to reference patterns that are available to determine what phases are present in the material under study. Figure 11 shows patterns of undoped and Ag doped ZnO thin films prepared by spray pyrolysis. A phase is a specific chemistry and atomic arrangement. However, phases with the same chemical composition can have drastically different diffraction patterns [54]. There are, however, instances where the XRD patterns are defective due to various reasons such as peak widening due to internal stress and defects [55].

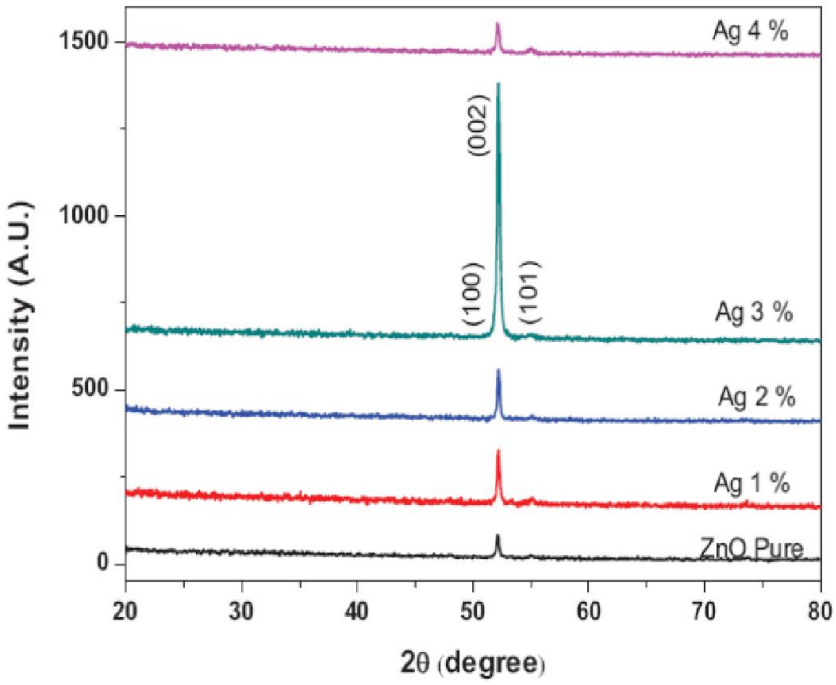

Figure 11: XRD patterns of undoped and Ag doped ZnO thin films prepared by spray pyrolysis onto glass (47: pg. 111)

2.6 Optical properties of composite thin films

The optical properties of noble-metal nanoparticles differ greatly from those of individual atoms [56]. Karamaliyev et al. [56] describe how these properties are related to collective vibrations of conductance electrons (plasma resonance) near the particle surface through the action of electromagnetic radiation. Bandgap is defined as the difference in energy between the valence band and the conduction band of a solid material (such as an insulator or semiconductor) that consists of the range of energy values forbidden to electrons in the material. An illustration of a bandgap is displayed in Figure 12 below. Various studies have evidenced that ZnO exhibits a wide band gap and for this reason it solely is unable to absorb light in the visible spectrum. Thus, various attempts of lowering the band gap of ZnO in recent years have been employed in order to improve its solar light harvesting capability [57]. There exist two types of bandgap semiconductors, viz. Direct band-gap (DBG) semiconductors and Indirect band-gap (IBG) semiconductors. According to Kittel and Ashcroft as cited by Seo et al. [58] “A band gap is said to be “direct" when the energy minimum (the bottom) of the conduction band lies directly above the energy maximum (the top) of the valence band in reciprocal k-space” (pg.23). A schematic representation of direct and indirect bandgap is shown in Figure 13. The maximum energy of the valence band is at a different value of momentum to the minimum in the conduction band energy in an indirect band gap semiconductor [59].

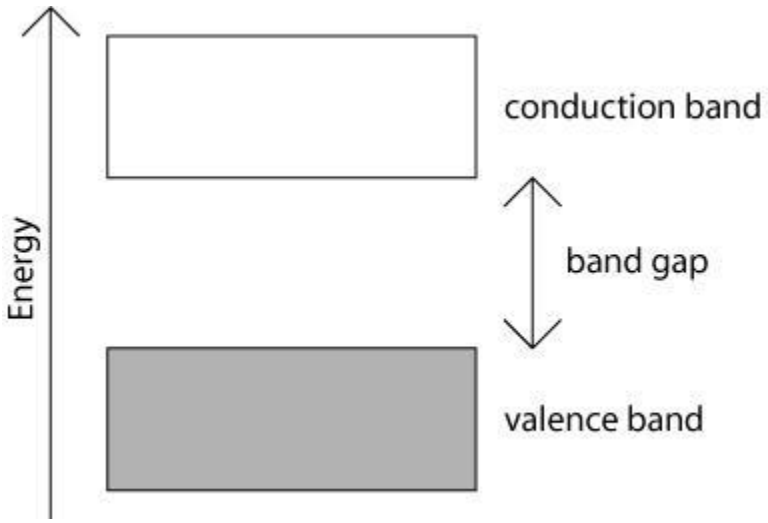

Figure 12: Band Gap illustration

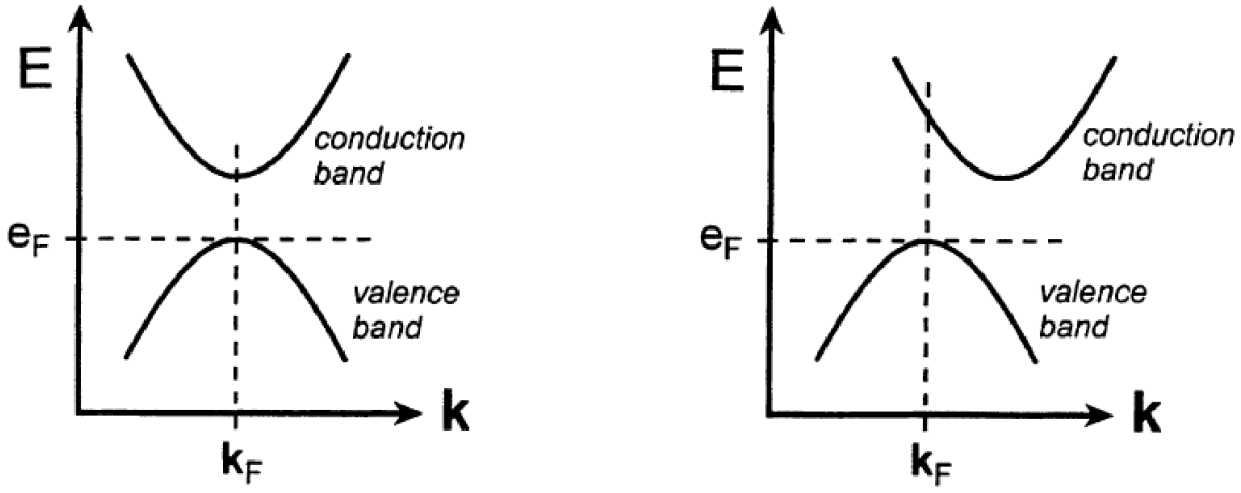

(a) (b)

Figure 13: Schematic representation of (a) direct and (b) indirect bandgap (56:pg 24)

The optical properties of ZnO are typically measured using spectrophotometric tools such as transmission spectra. An optical study conducted by Purica et al. [60] found that films showed high transmission in the near-infrared and visible region with a steep fall-off in transmission at approximately >400 nm. They further conducted bandgap studies on ZnO in which they obtained an energy gap (*Eg*) of 3.47 eV for deposited films compared to a value of 3.2 eV for ZnO bulk semiconductor [60]. The bandgap of ZnO was found by the extrapolation of a plot of $(\alpha hv)^2$ vs. (*h*v) to zero absorption coefficient in the range where band–band absorption of the radiation begins. Figure 14 below shows the optical and bandgap studies done on ZnO thin films.

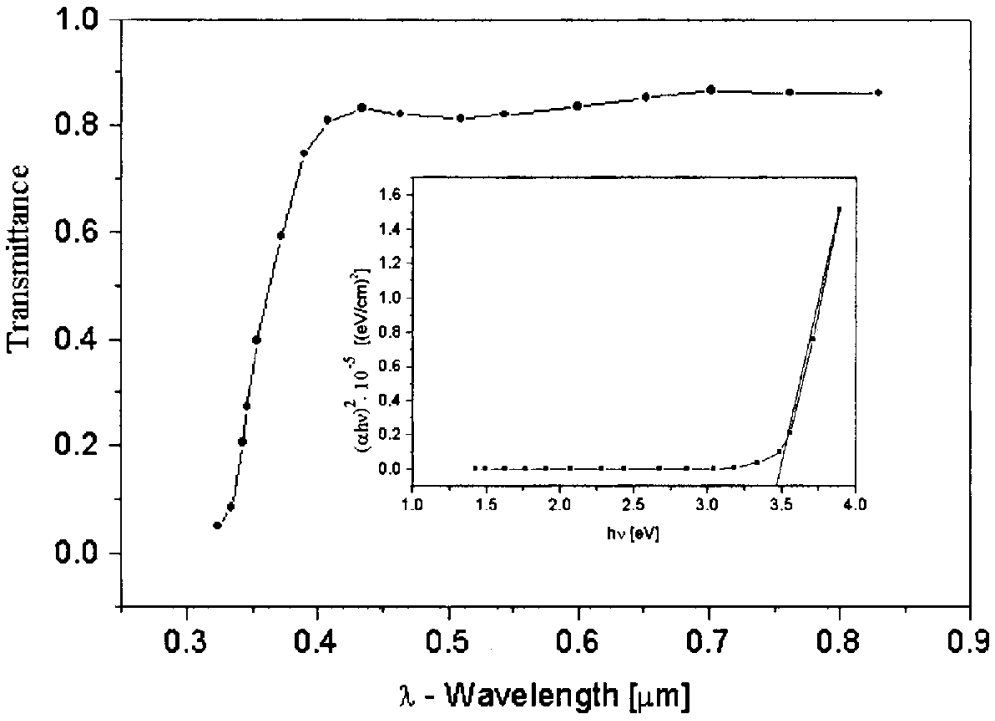

Figure 14: Optical and bandgap studies done on ZnO thin films (60: pg. 488)

The optical structure of ZnO when combined with composites such as Ag has also been extensively studied. The Ag-nanoparticles were prepared by the spontaneous reduction method with Ag 2-ethylhexanoate and the XRD patterns [61] of ZnO doped with Ag-nanoparticles annealed at 700

°C is shown below. Hong et al. [61] explain that “In this investigation, the introduction of Ag nanoparticles did not affect the crystallization of ZnO films. This may be due to the presence of trisodium citrate, a capping agent for the size control of Ag-nanoparticles” (pg.958). Research suggests that the use of a capping agent such as trisodium citrate minimizes the effect of Ag-nanoparticles on the nucleation of ZnO [61].

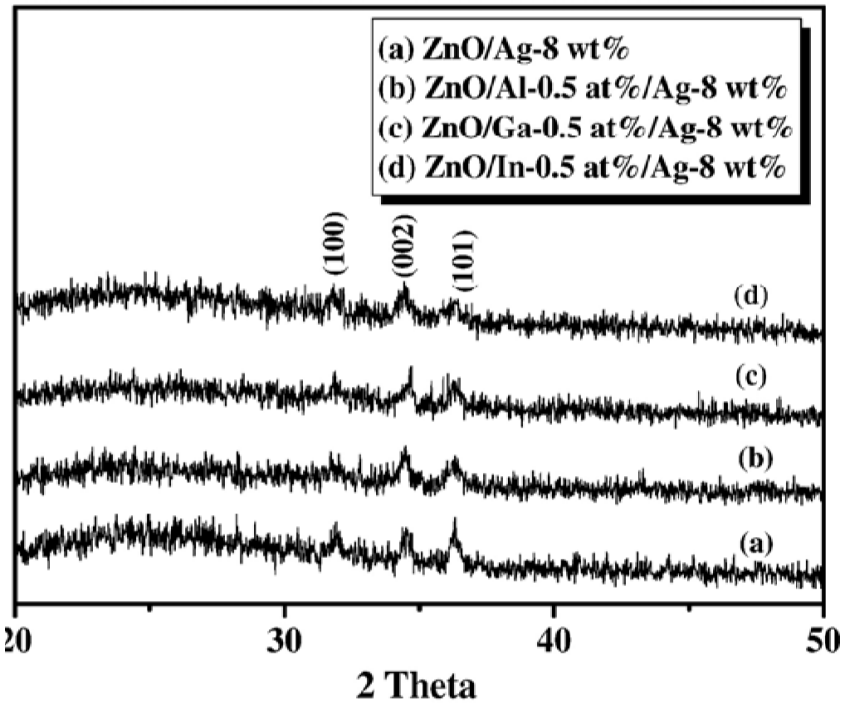

Figure 15: XRD patterns of ZnO doped with Ag-nanoparticles (61: Pg. 958)

2.7 Photocatalytic study of modified ZnO thin films

Heterogeneous photocatalysis is an economical alternative and environmentally safe technology of advanced oxidation processes for the removal of organic impurities from water. During that process, the semiconductor illuminated by light of the proper wavelength absorbs light and

generates active species, which oxidize the organic compounds dissolved in water. One of the promising materials for this application is ZnO because of its high chemical stability, nontoxicity and high electron transfer capability. Several researchers reported that modification of the ZnO surface with metals like Sn, Cd, Mn and Cu is promising as a tool to enhance its photocatalytic activity [62]. In particular, silver as a noble metal deposited on ZnO substrate (Ag/ZnO) has attracted considerable attention for its remarkable role in the improvement of the photocatalytic activity of semiconductors. Silver can also be reused and handled more easily and economically if impregnated on substrates [30]. Therefore, an attempt has to be taken to shift the threshold of the photo-response of ZnO into the visible region through doping with Ag-nanoparticles.

A photocatalytic study was done on methyl violet, where it is fed as a groundwater pollutant and its destruction helps to remove pollutants [63]. Various factors affect how effectively ZnO nanoparticles will remove insoluble chemicals, and those include oxygen vacancy, surface properties such as surface area, and hydroxyl ions [64]. According to studies, the photocatalytic activity of ZnO nanoparticles under UV light show enhanced activity and doping with silver improved the photocatalytic activity with an optimum 2%, which may be related to the oxygen vacancy defect concentration [63]. Hosseini et al. [63] further speculate that "Increasing Zn vacancies accompanied by oxygen vacancies could be responsible for the degradation process" (pg. 8). The decolourisation of the dye can be attributed to the reaction between conduction-band electrons and oxygen in the solution to generate the reactive oxygen species [65]. Amornpitoksuk et al. [65] clarify that "the electron hole pairs (e_{cb}^{-}/h_{vb}^{+}) in ZnO are generated when it absorbs the photon with an energy equal to or higher than the energy band gap of the ZnO" (pg. 162). Superoxide anion radicals ($\bullet O_2^{-}$) are produced when the photogenerated electrons react with

oxygen species while the photogenerated holes react with water molecules to generate hydroxyl radials (•OH) [65]. The produced reactive radicals work together coherently to decompose/decolorize organic compounds. Figure 16 below shows the photocatalytic degradation of methylene blue as a function of irradiation times on Ag-doped ZnO powders with different Ag contents as well as the effect of the Ag concentration on the photo degradation reaction after 1 h of irradiation.

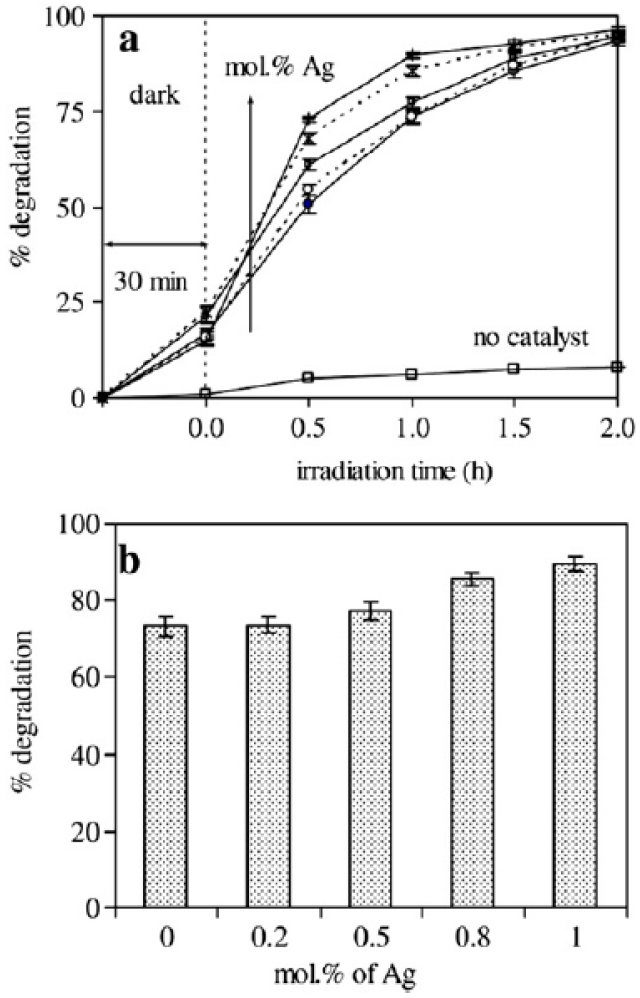

Figure 16: (a) Photocatalytic degradation of methylene blue as a function of irradiation times on Ag-doped ZnO powders with different Ag contents (b) The effect of the Ag concentration on the photo degradation reaction after 1 h of irradiation (65: pg. 162).

A summary of the primary reactions that occur when a semiconductor is excited upon received minimum photon energy in the presence of O_2 and H_2O is summarized in Figure 17.

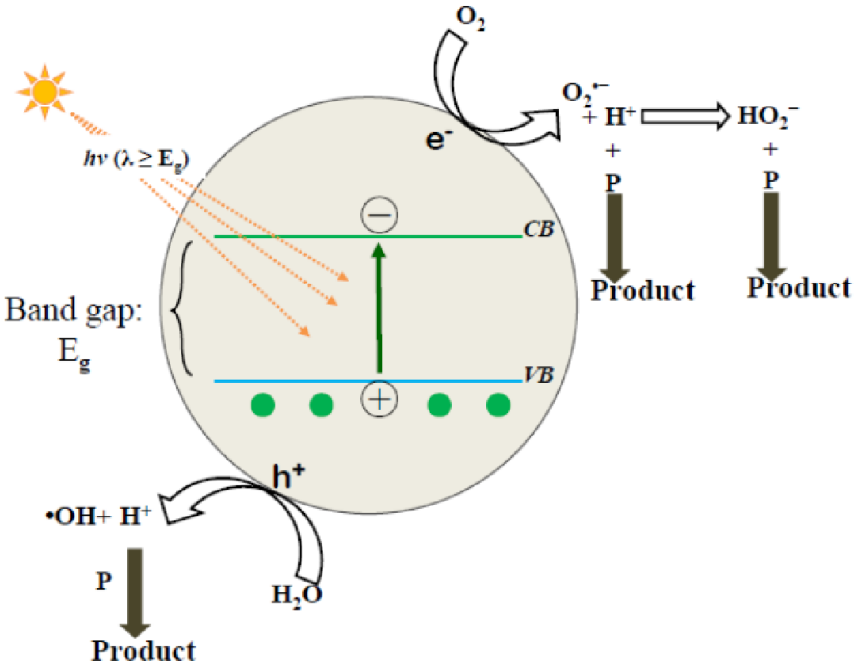

Figure 17: Reactions that take place in a semiconductor (30: pg. 9)

Chapter 3: Research Methods

3.1 Research design

Using MPM, a coating precursor solution of ZnO and Ag was prepared. The precursor solution was coated on a glass substrate using a spin coater. Homogeneous distribution and growth of Ag-NP in the composite thin films were determined using X-ray diffraction (XRD). The absorption spectra of the thin films were studied using UV/Vis spectrometer. The electrical conductivity of the thin films was investigated using the 4-probe method. The photocatalytic activity of pure ZnO and composite thin films were estimated by measuring the decomposition rate of Methyl orange (MO) in an aqueous solution containing the thin films as photocatalysts. Figure 18 shows the research design that was undertaken.

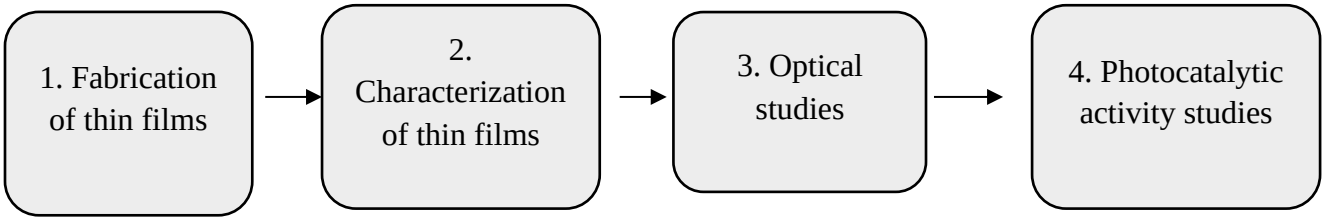

Figure 18: Research Design

3.2. Procedure

3.2.1 Preparation of ZnO precursor solution

A precursor solution of zinc oxide was prepared by reacting zinc acetate dihydrate with dibutylamine and ethylenediaminetetraacetic acid (EDTA) in a mixture of ethanol and methanol, whereby ethanol and methanol acted as the solvent. Finally, hydrogen peroxide was added and a clear solution resulted. In element, 3.6238 g EDTA was dissolved in 4.62 mL dibutylamine and a

mixture of 12.63 mL methanol and 12.67 mL ethanol were added to the dissolved EDTA. The contents were then transferred into a round bottomed flask and heated under reflux for 30 min to completely dissolve the solids. Thereafter, the resulting solution was allowed to cool to room temperature and 2.7218 g Zinc acetate dihydrate was carefully added to the flask, then further heated under reflux for 2 hours and 30 minutes. Finally, the solution was allowed to cool and 0.4660 g hydrogen peroxide solution was added, then a final heated reflux of 30 min was allowed before obtaining the clear solution which was then used as a zinc oxide precursor solution. The flow diagram below in Figure 19 shows the preparation of ZnO precursor solution.

3.6238 g, 12.4 mmol EDTA

4.62 mL dibutylamine

12.63 mL Methanol + 12.67 mL Ethanol

Heat under reflux, 30 min

Cool to room temperature (r.t)

2.7218 g, 12.4 mmol $Zn(CH_3COO)_2 \cdot 2H_2O$

Heat under reflux, 2H30

0.4660 g, 13.7 mmol H_2O_2

Heat under reflux 30 min, cool to r.t

Heat under reflux 30 min, cool to r.t

12.4 mmol Zinc precursor

Figure 19: Flow chart showing the steps employed in preparing the 12.4 mmol zinc precursor solution

3.2.2 Preparation of Ag precursor solution

The silver precursor solution was simply prepared by dissolving 0.2337 g silver acetate in 0.72 mL dibutylamine and 1.28 mL ethanol by stirring on a magnetic stirrer for 5 minutes. The solution prepared was used immediately to make the composite precursor solutions of ZnO and spin coat. Figure 20 below shows in detail the preparation of the silver precursor solution.

0.2337 g, 1.4 mmol Silver Acetate

0.72 mL,4.3 mmol Dibutylamine

1.28 mL EtOH

Stir for 10 minutes on magnetic stirrer

1.4 mmol Silver precursor solution

Figure 20: Flow chart showing the steps employed in preparing the 1.4 mmol Silver precursor solution

3.2.3 Fabrication of ZnO and Ag-NP/ZnO composite thin films using the Molecular Precursor Method

The Ag-NP/ZnO thin films were prepared by the MPM spin coating technique using a precursor of zinc, namely, zinc (II) acetate dihydrate ($Zn(CH_3COO)_2 \cdot 2H_2O$) and a Ag precursor. Precursor films were deposited on the quartz glass substrate at ambient temperature using the spin-coating

method, in a double-step mode: the first step was carried out at 500 rpm for 5 s and the second, at 2000 rpm for 30 s, for all preparations. Two thin films of Ag nanoparticles and zinc oxide were formed by heat treating the spin-coated precursor films and applying the precursor solutions of silver and zinc, respectively. The Ag-NP/ZnO composite films were fabricated by heat treating the spin-coated precursor films, while applying the solution Ag/ZnO composite, at first pre-heated at 200 ºC, then finally heat treated at 600ºC in air to eliminate organic ligands from metal complexes involved in spin-coated precursor films using the spin-coating method [7]. The number *n* in the notation of the composite films indicates the silver molar percentage (Ag mol%) to ZnO; for example, the name Ag 40 indicates that the silver molar percentage in the Ag/ZnO composite solution was 40 mol%. The fabricated thin films were clearly labelled to prevent mix up as they all fairly looked the same in color. Scheme 1 below details the procedure for fabricating thin films by MPM.

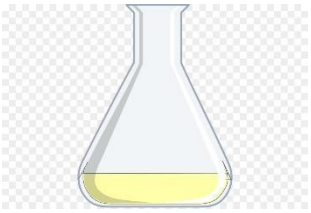

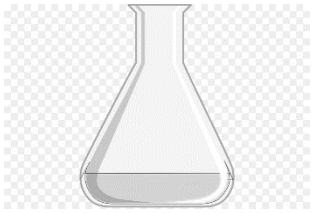

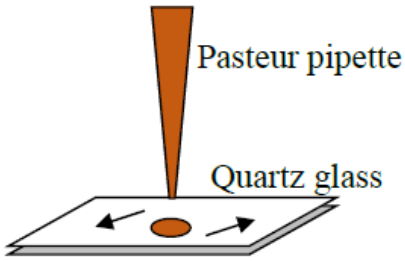

olution

ecul

s

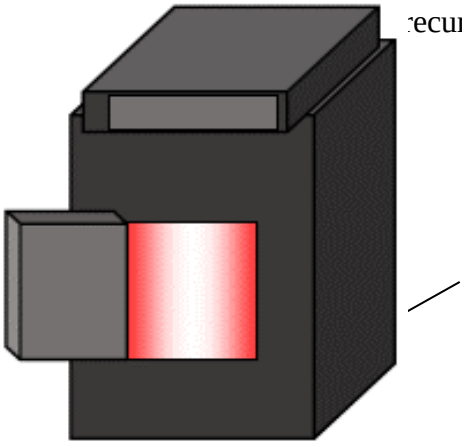

Coated precursor thin film

Fabricated thin film

Heat treatment at 600 °C

Scheme 1: Procedure for fabricating thin films by MPM

3.2.4 X-ray diffraction (XRD)

The characterization of the atomic structure of a thin film at large scale, XRD technique appears as the most powerful method. Thus, in this thesis, the X-ray diffraction (XRD) patterns of Ag particles, ZnO, and Ag-NP/ZnO composite thin films were measured using an X-ray diffractometer (MXP-18 AHF22, Bruker AXS) with Cu–Kα rays generated at 45 kV and 300 mA. Parallel beam optic was employed with an incident angle of 0.3º.

3.2.5 Determination of the optical properties of the fabricated thin films

The absorbance spectra of pure ZnO, pure Ag as well as for those of the Ag-NP/ZnO composite thin film samples were performed with a The Perkin Elmer Lambda 35 UV/Vis spectrometer provided with a diffuse reflectance accessory.

3.2.6 Calculation of band gap using absorption spectra of Ag-NP/ZnO thin films fabricated on quartz glass substrates

The optical band gap, Eg, of the ZnO and Ag-NPs/ZnO composite thin films was calculated using the following Tauc expression:

$$\alpha = \frac{A(Ephot)-A(Egn)}{E(phot)} \text{.....3.1.1}$$

where E_{phot} (hv) is photon energy equal to 1239/λ (eV), A is a constant, and α is the absorption coefficient at a given wavelength (nm), and n is equal to 0.5 by considering values for the direct mode of transition.

3.2.7 Investigation of the photocatalytic reduction of Methyl orange by Ag-NP/ZnO composite thin films

The photocatalytic activity of pure ZnO and composite thin films were estimated by measuring the decomposition rate of MO in an aqueous solution containing the fabricated thin films as photocatalysts under visible light and under dark. The doped and undoped ZnO thin films were used as the photocatalysts. The concentration of the MO was calculated using a simplified equation derived from the Beer Lambert Law:

$$A = \varepsilon cl \quad \text{..... 3.2.1}$$

where A is the absorbance, l is the path length in cm, ϵ is the molar extinction coefficient having unit L $mol^{-1}cm^{-1}$, and c is the concentration in mol L^{-1}. The absorbances used were derived at the same wavelength of 465 nm and thus this simplified formula was used to determine the final concentration of the MO after decomposition by the photocatalysts quantitatively:

$$\frac{C1}{C2} = \frac{A1}{A2} \quad \text{..... 3.2.2}$$

The decoloration rate of MO by each thin film was determined by calculating the index of photocatalytic activity (IPCA). The initial decoloration rate (k) values of concentration after t minutes of 0.02 mM MO aqueous solution by photoreaction with each potential photocatalytic thin film and a blank were measured by an approximate line for the function of C(t) *versus* t obtained in the range from $0 \leq t \leq 180$ min by a least-squares method [7].

$$IPCA = 10^3 \, x \, \frac{kn}{3} \quad \text{..... 3.2.3}$$

Photocatalytic activity of pure ZnO and composite thin films was estimated by measuring the decomposition rate of methyl orange (0.02 mM) in an aqueous solution (20 mL) containing 20 ×

20 mm^2 thin film photocatalyst. Various Ag-NP/ZnO composite thin films with different Ag molar concentration or pure ZnO thin film were used as the photocatalysts. The photocatalysts were immersed in the 0.02 mM MO aqueous solutions for 8 hours in the dark to allow equilibrate adsorption on the film surfaces. The photocatalysts were then also immersed in the same solution for 8 hours under visible light (sunlight) to study the effects of photo degradation of the MO solution under visible light. The MO concentration was determined by measuring the absorption spectra of the aqueous solution with the PerkinElmer Lambda 35 UV/Vis spectrophotometer. For the decomposition test, 3 mL of the 0.02 mM MO aqueous solution was transferred into a quartz cell of dimensions 1 W × 1 L × 4.5 H cm^3 at 20 min intervals. After spectral measurement, the solution was immediately returned to the vessel and mixed with the aliquot. The mixed solution continued to be used until the test for each film was completed. The mixed solution was further used until the test for each film was done again after 8 hours. The absorption peak value at 465 nm were used in order to determine the concentration of MO after t minutes, C(t), using equation 4:

$$C(t) = 10x\ \frac{abs\ (t)}{abs\ (0)} \quad \text{.....3.2.4}$$

where Abs(0) and Abs(t) represent the absorption values of the solution just before the light irradiation and after t minutes during irradiation, respectively. The pseudo-first-order kinetic constant (k) values of concentration after t minutes of 0.02 μM MO aqueous solution by photoreaction with each specific photocatalyst and a blank were measured by an approximate line for the function of C(t) versus t obtained in the range from $0 < t < 480$ min by least-squares method. The amounts of methyl orange that remained was examined three times for each film, and the index of photocatalytic activity (IPCA) of the film was estimated from the averaged value of the pseudo-first order kinetic constant, using equation 3 [30].

4. Research Ethics

All waste generated in the laboratory were disposed of in clearly labelled waste containers. In addition, organic and inorganic wastes were separated accordingly. The containers were then collected and disposed of by a specialist contractor in order to meet safety, health and legislative requirements. The guidelines for waste disposal of the UNAM Standard Operation Procedure document number SOP-29-1 and UNAM Occupational Safety and Health guidelines were also considered. Ethical clearance was obtained from the UNAM Research Ethics Committee and research permission was obtained from the Centre for Post-Graduate Studies before commencement of the study.

Chapter 4: Results and Discussion

4.1 Preparation of the precursor solutions

The precursor solution for fabricating silver films were obtained by dissolving an appropriate amount of silver acetate in ethanol in the presence of dibutylamine. Figure 22 below shows the zinc precursor prepared. The zinc precursor solution prepared was a clear, stable solution, MPM precursor solutions are stable and can be still used after a year compared to sol-gel solution which must be used immediately as it turns into a gel. Similarly, the silver precursor solution was a clear to light grey colour; it was also found to be unstable due to the photochemical activity of silver.

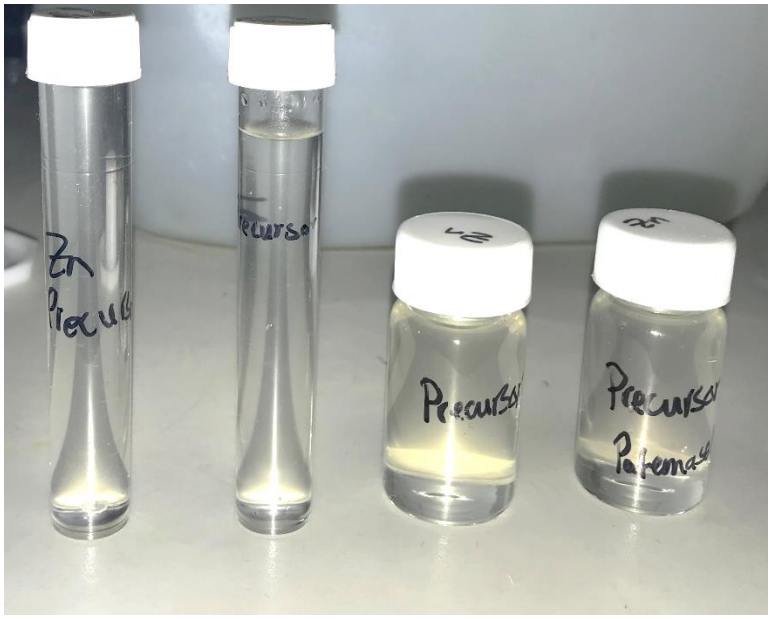

Figure 22: Zinc Precursor Solution

4.2 X-Ray structures of the fabricated thin films

4.2.1 X-ray structures of pure ZnO and Silver fabricated thin films

Figure 23 shows XRD patterns of the films fabricated at 600ºC applying the zinc complex and silver acetate solutions, respectively, from which it was elucidated that the resultant pure silver

and pure zinc oxide films contain silver crystallized in the cubic system [JCPDS card 4-783, 1978] and zinc crystallized in the c-axis (002) orientation system [JCPDS card 21-1272, 1978; JCPDS card 21-1276, 1978], respectively.

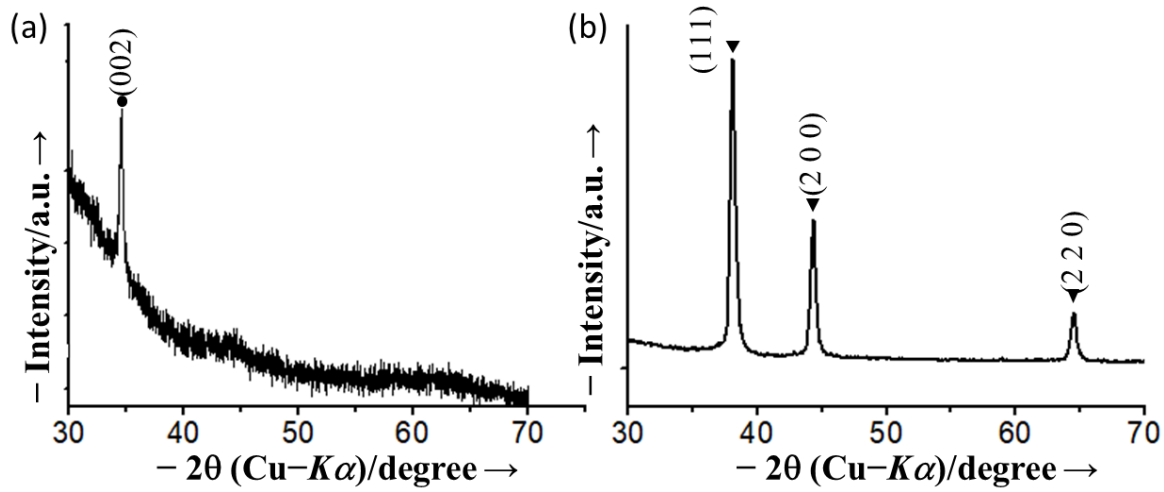

Figure 23: XRD of (a) ZnO and (b) Silver thin films heat treated at 600 °C and fabricated by MPM. The peaks of each phase are denoted as follows: filled circle ZnO, and filled inverted triangle metallic silver

The ZnO thin film shows no peaks in the XRD spectrum except a peak found at 2θ = 37.5°, corresponding to the [002] plane [JCPDS S6-314], which shows that the fabricated ZnO thin film is highly c-axis oriented as the kinetically favored, which is of interest for piezoelectric application such as the photocatalytic and photovoltaic studies. According to literature, [002] diffraction peak has been observed widely for the ZnO materials that preferred such an orientation and its appearance suggests that the surface free energy of this plane is the lowest in the MPM employed to fabricate this film. Weak peak in the spectrum of ZnO might be due to the small grains of ZnO [30]. The peaks at 38.18, 44.39, and 64.58° are assigned as the (111), (200), and (220) reflection

lines of fcc Ag particles (JCPDS file, No. 04-0783), respectively [JCPDS card 4-783]. Sharp diffraction peaks indicated the formation of pure silver of high crystalline [30]. Moreover, no inessential peaks appeared under the heat treatment, as only peaks for Ag metallic were detected and there was no indication of the presence of silver oxide, which is mainly observed at 36.5° [JCPDS card 40-909]. Thermodynamics studies have suggested that silver is more stable than Ag_2O/AgO at temperatures above 189.8 °C in air [30]. Therefore, any of Ag_2O/AgO that is present decomposed to metallic silver during heat treatment at 600°C.

4.2.2 X-ray structures of the fabricated Ag-NP/ZnO composite thin films

Figure 24 shows XRD patterns of Ag-NP/ZnO composite thin films, with various molar concentration of silver particles in ZnO matrix, deposited on quartz glass substrates and heat treated at 600°C for 30 min.

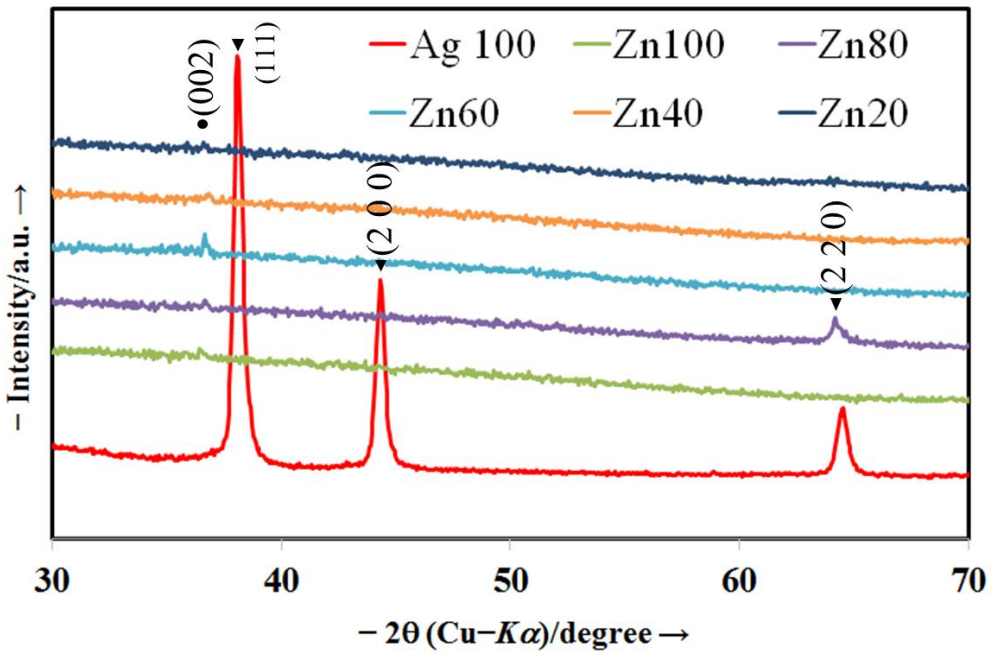

Figure 24: The XRD patterns of the Ag-NP/ZnO composite thin films various Ag molar concentration in a ZnO matrix. The peaks are denoted as follows: filled inverted triangle silver and filled circle ZnO

Except for the extremely small peaks of silver (the peak at 2θ = 64.58°) that appeared in the composites of Zn 80 (Ag 20%) the XRD spectra indicate that no other Ag peaks were present in the composite thin films. This indicates that no reaction took place between ZnO and silver during heat treatment. The silver peak appeared in the XRD patterns of the Ag-NP/ZnO composite thin films at the highest Ag content 80 mol% may have formed during the cooling stage [33]. As reported in the pure ZnO spectra in Figure 24 above, a single peak at 2θ = 37.5° can also be observed in the composite. This illustrate again that the [002] diffraction peak is due to the kinetically favoured orientation in the crystallization of ZnO [30]. It is well known that the crystalline phase adopted by ZnO is mainly dependent on method of fabrication, hence, under the current conditions, Ag/ZnO composite thin film are obtained at 600°C are c-axis oriented.

4.3 Optical study of fabricated thin films

4.3.1 Absorption spectra of ZnO and Ag NP thin films

The UV-Vis absorption spectra of the pure ZnO and the composite AgNPs/ZnO was studied in the visible wavelength region of 300 – 700 nm. Figure 2 (a) and (b) represent the UV-Vis absorption spectra for pure ZnO and Ag thin films. The ZnO thin film showed a low-intensity absorption band in the visible region; however, its absorption intensity increased steeply at shorter wavelengths (UV-region).

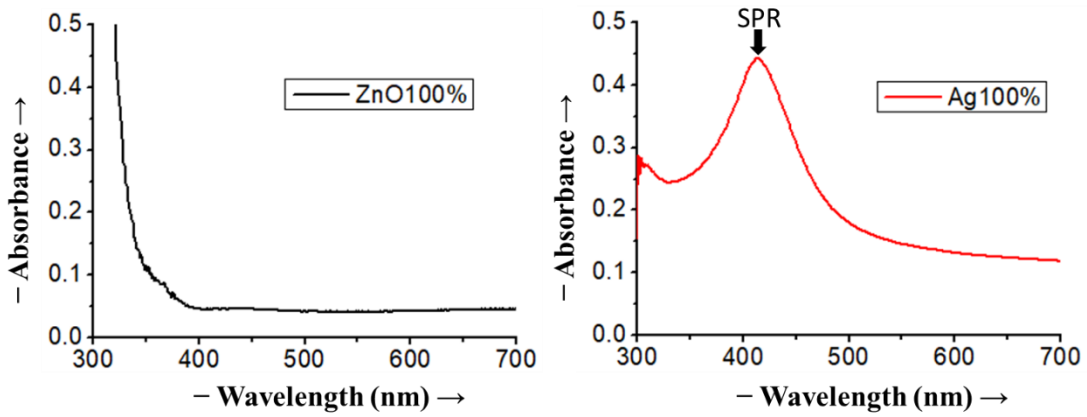

Figure 25: Absorption spectra of the fabricated thin films: (a) pure ZnO thin film and (b) pure Ag thin film, respectively.

In contrast, the Ag NP film showed a weak and broad absorption band at around 410 nm. A large oscillating electric field is observed around the metal particles when a Ag NP film is irradiated with visible light [35]. The absorption band in this region corresponds to the characteristic surface plasmon resonance (SPR) of AgNPs. Theoretically, according to Likius [30], large oscillating electric fields are formed around and among the metal nanoparticles because of localized surface plasmon resonance (LSPR) when samples are irradiated by visible light.

4.3.2 Absorption spectra of AgNP/ZnO composite thin films

The UV-Vis absorption spectra for the Ag-NP/ZnO composite thin films (20, 40, 60 and 80 %) are shown in Figure 26. The intensity of absorption maximum in the visible region increased with an increase in the Ag content in the ZnO matrix, hence an increase in the SPR peak. This increase in the SPR absorption intensity can be attributed to the decrease in the amount of ZnO, hence the thin

films become more metallic. Therefore, the absorption maximum observed in the visible region can be due to the characteristic LSPR for the Ag NPs incorporated in the ZnO matrix.

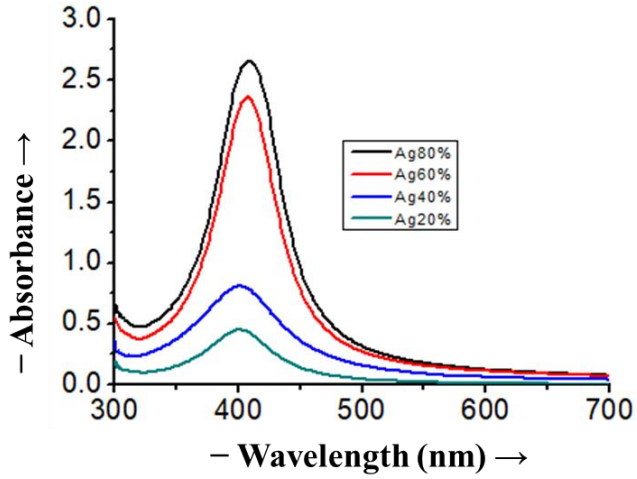

Figure 26: UV–Vis absorption spectra for Ag-Np/ZnO composite thin films fabricated on quartz glass

The absorbance spectra maximum of the synthesized Ag-NP/ZnO composite thin films are increasing with the molar concentration of silver in zinc oxide, indicating that the silver nanoparticles are capable of sensitizing ZnO. Therefore, the Ag-NP/ZnO composite thin films can be activated by visible light to generate electrons and holes, which is favorable to the improvement of the visible light photocatalytic activity of ZnO. This means that the AgNPs also affect the band gap of the semiconductor, ZnO, through doping. In order to validate this, the band gap of the composite thin films was studied.

4.4 Band gap determination

The band gap of ZnO and Ag-NPs/ZnO thin films was determined by plotting (absorbance)^2 vs photon energy and extrapolating the linear portion of the curve to the photon energy axis, as shown in Figure 27. The band gap energy (in eV) is obtained by extrapolating the straight-line portion of the plot to the zero absorption coefficients. Extrapolating the optical band gap of the pure ZnO thin film, an E_g value of 3.3 eV was obtained, which is in fact equal to the band gap of pure ZnO (assuming direct transition). However, the band gap for the AgNP/ZnO composite thin films fabricated using MPM were quite a bit lower; the band gap for Ag 20, 40, 60, and 80 % are summarized in Table 1 and are shown in Figure 27 (b). Thus, the incorporation of AgNPs into the ZnO matrix did affect the band gap of ZnO.

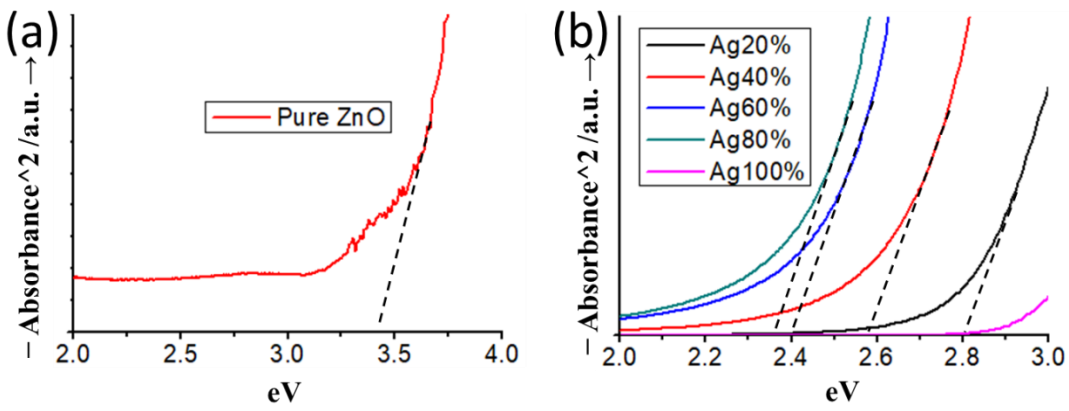

Figure 27: Plots of [absorbance]^2 versus photon energy of: (a) ZnO thin films and AgNP/ZnO composite thin films

Table 1. Band gap values of fabricated thin films

Thin film	Pure ZnO	Ag20%	Ag40%	Ag60%	Ag80%
Band gap (eV)	3.3	2.8	2.6	2.4	2.3

Since the extrapolating optical band gap of the composite films which is not equal to that of pure ZnO validate that the ZnO band gap changed with incorporating silver into ZnO thin film. These films could still easily absorb photons to produce photoexcited electrons under both UV and visible light because they had a band gap less than that of pure ZnO. Owing to this band gap, they could respond to UV light and show characteristic absorptions due to SPR caused by visible light. Therefore, all these thin films have the potential to act as photocatalysts.

There is a clear decreasing trend in bandgap energy with an increase in AgNPs content in the thin film. Furthermore, this significant increase in band gap due to the addition of AgNPs ties to the photo response activity of ZnO in the visible region of the electromagnetic spectrum. This also supports literature in the sense that ZnO alone does not respond to visible light alone, however only when doped with a noble metal such as silver. ZnO due to its metallic properties and wide band gap only responds in the UV region of the spectrum. Therefore, the decrease in band gap energy by doping with AgNPs proves theory right.

4.5 Photocatalytic Activity of Thin Films

4.5.1 Decomposition of MO dye under visible light (sunlight)

Figure 28 below demonstrates the decomposition of MO dye under visible light by the fabricated thin films. There was no visible change observed in the intense orange colour of the MO dye.

Figure 28: Decomposition of MO under visible light

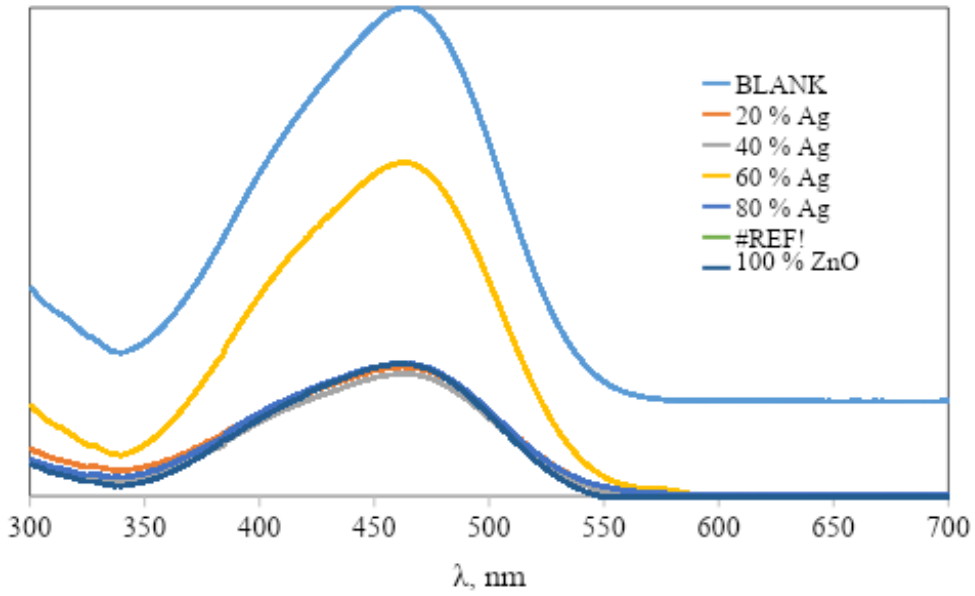

Figure 29: Absorption spectra of decomposition of 0.02 mM of MO aqueous solution in the presence of different Ag-NP/ZnO thin films after kept under visible light (sunlight) for 8 hrs

Figure 29 represents the UV-vis absorption spectra of ZnO and AgNPs under visible light irradiation. The effect of decomposition of the MO dye by the thin films by comparing the initial concentration of the MO (Blank) with the final concentration after decomposing for 8 hours under visible light was studied. Studying the absorption spectra carefully reveal that all AgNPs/ZnO

composite thin films decrease the concentration of the MO dye to a certain extent. However, it is evident that the 40% Ag composite film significantly decreases the concentration from 0.02 mM to 0.00499 mM. Table 2 below shows the decrease in concentration of the MO dye by decomposition of the composite films. The absorption spectra of the 20%, 40% and 80% AgNP/ZnO composite thin films show a significant decrease in the concentration of MO dye compared to that of 60% AgNPs. It is also observed that the 100% ZnO thin film, without compositing with AgNPs, decreases the concentration of MO to a certain extent and this decrease can be due to self-absorption of the MO solution. Furthermore, the decrease in concentration of MO can be attributed to compositing ZnO (a wide band gap conductor) with Ag metal that exhibits plasmonic properties.

Table 2. Decomposition of MO under sunlight by composite films

Thin Film	[MO] final, mM	[MO] initial, mM
20% Ag	0.00527	0.02
40% Ag	0.00499	0.02
60% Ag	0.01361	0.02
80% Ag	0.00541	0.02
100% ZnO	0.00539	0.02

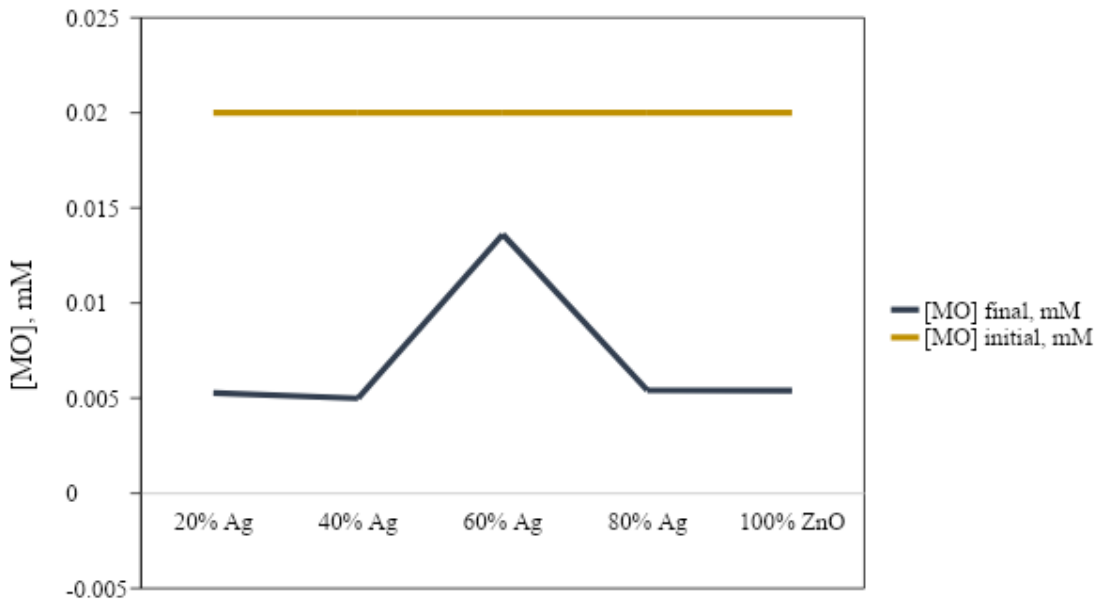

Figure 30: Decrease in concentration of MO via decomposition by thin films under visible light

Figure 30 above better reveals the extent to which the concentration of the MO dye was decreased is significant and this also proves that silver is a good noble metal for doping with ZnO to improve the photo response activity of ZnO. The 40% AgNPs thin film showed to have the most decrease in the concentration of the MO dye and this may have been due to the decrease in the concentration of wurtzite in ZnO as well as the decrease in ZnO in the composites by increasing the Ag content [30]. The 60% AgNPs thin film proved to have the least impact on decreasing the concentration of the MO dye and this could be caused by an experimental artefact such as introduction of errors by contamination of the vial that contained the solution or instrumental errors at the time of analysis. Literature suggests that the visible-light-responses are due to the electron donor levels in the band gaps formed by doped transition metal ions, in this case silver.

4.5.2 Decomposition of MO dye under dark conditions

The Ag-NPs/ZnO thin films were similarly immersed in 0.02 mM MO for 8 hours under dark conditions, safeguarding that there was no passage of light through to the petri dish. The same procedure as under visible light was followed; where after 8 hours the thin films were removed from solution and the solution was analysed by UV-Vis spectrophotometer to determine the absorption spectra of each solution that contained the different composite films. Figure 31 below shows the decomposition of MO dye under dark conditions.

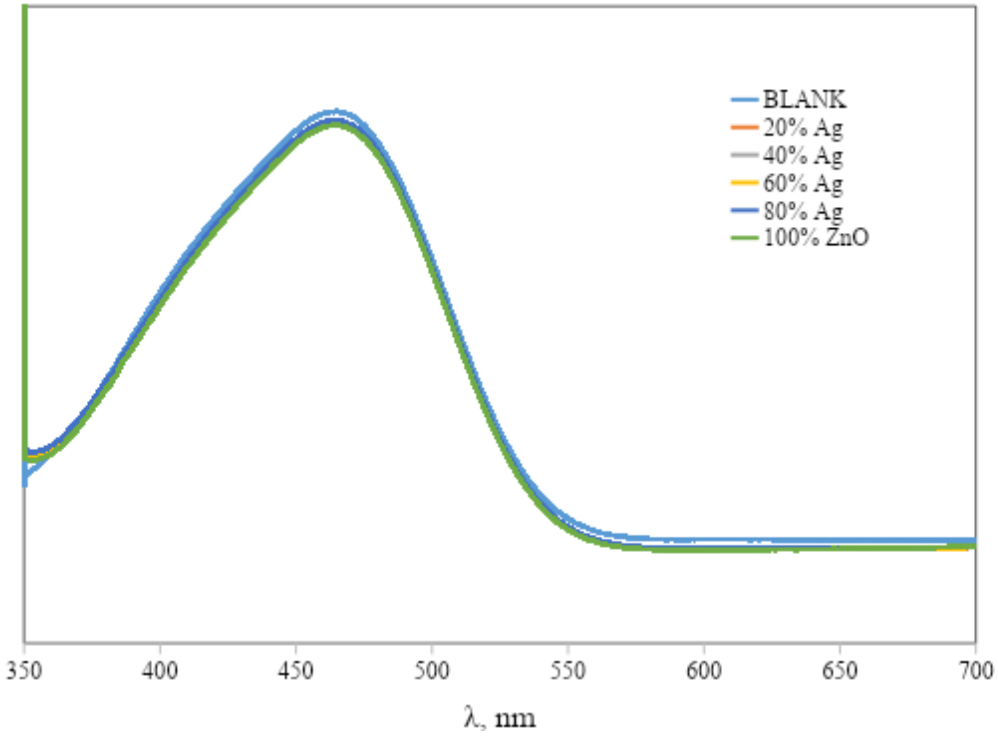

Figure 31: Absorption spectra of decomposition of 0.02 mM of MO aqueous solution in the presence of different Ag-NP/ZnO thin films after kept under dark conditions for 8 hrs

The data obtained reveal that there was an insignificant decrease in concentration of the MO concentration when compared to the effect of visible light. This is attributed to the fact that the decomposition of the dye is only effective under visible light where photo reactions take place.

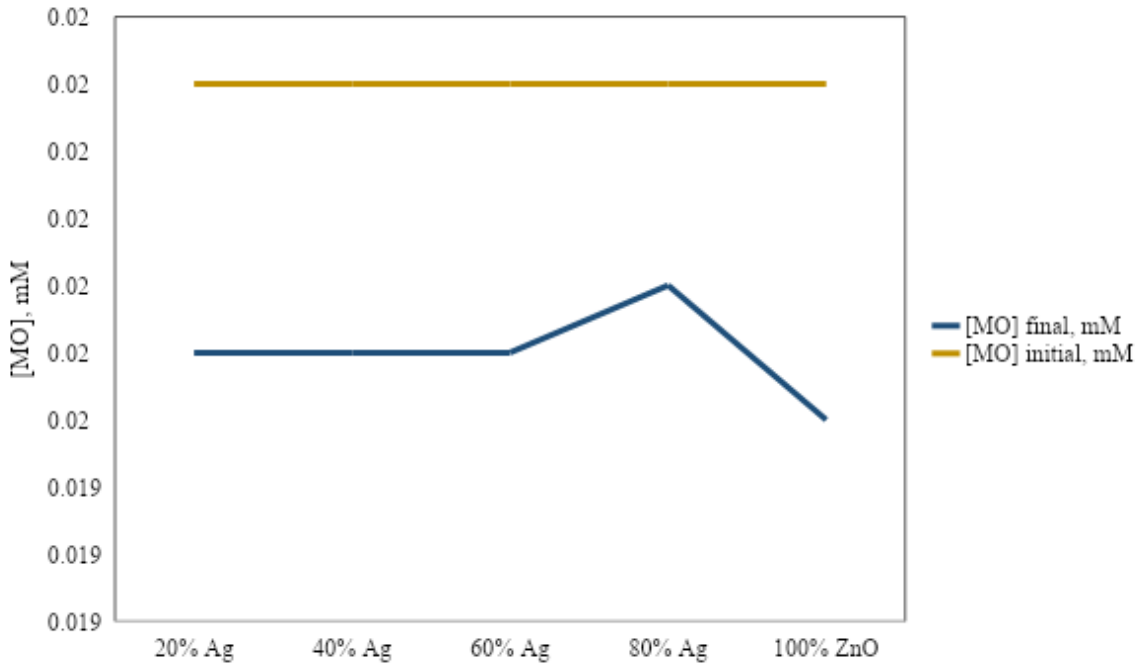

Figure 32: Decrease in concentration of MO via decomposition by thin films under dark conditions

There was no significant decrease in the concentration of the MO dye as can be seen in Figure 32 above.

Qualitative data was obtained by determining the Index of Photocatalytic Activity (IPCA, nM min^{-1}) of the decoloration rate of 0.02 mM MO solution to directly compare the performance of pure ZnO and composite thin films under light irradiation to the dark condition. The experiment was only conducted once and the results produced were within narrow limits. The IPCA values

extracted from a decoloration rate of 0.02 mM MO solution by photoreaction with each composite thin film and a blank are displayed in the Table 3 below.

Table 3. The index of photocatalytic activity (IPCA) of decoloration rate of 0.02 mM MO

	IPCA/nM min^{-1}	
Thin film	Visible Light	Dark
20% Ag	3.14	1.26
40% Ag	3.16	1.26
60% Ag	3.07	1.26
80% Ag	2.91	1.27
100% ZnO	7.94	1.25

Under visible light irradiation, none of the composite samples exhibit more photoactivity than the 80% Ag composite thin film, followed by the 60% Ag. Under dark, the IPCA for all thin films is more or less similar and not very effective as can be seen by the large values, additionally, the IPCA under dark condition can be representing both adsorption and self-decoloration of the dye MO [30]. The IPCA of the 100% ZnO is high under visible light and this is because ZnO as a semi-conductor does not exhibit plasmonic photocatalyst properties associated with Ag nanoparticles [30]. The different results reveal that the photoactive enhancement mechanisms under visible light irradiation and dark are different and that under visible light the photocatalytic activity is greatly enhanced.

5. Proposed mechanism for photocatalytic properties of plasmonic AgNP/ZnO composite thin films

The absence of wavelength shift near the absorption edges of the pure ZnO thin film in the spectra for the present Ag NP/ZnO composite thin films (shown in Figure 27 (a) and (b)), demonstrates

that there was a change in the band gap of ZnO by the addition of AgNPs. Furthermore, the UV-Vis absorption spectra showed that the well-defined SPR peaks and wide-range LSPR bands due to AgNPs are capable of efficiently sensitizing the AgNP/ZnO composite thin films. A plasmonic photoelectrochemical mechanism for the visible light absorbance by Ag NP/ZnO composite thin films prepared by MPM is proposed. This mechanism is illustrated by three steps in Scheme 1 below. Daniel [30] explains that "(1) Due to LSPR, electrons from the Ag NPs are promoted to higher states in the band; (2) These electrons are then injected into the conduction band of TiO_2, provided they have sufficient energy; and, (3) The photoexcited electrons then travel faster through the electrolyte to counter electrode, producing a cathodic photocurrent" pg. 223. Using this same concept, a mechanism for the AgNP/ZnO composite thin films was developed. An anodic photocurrent can only be generated if the potential initiating at the counter electrode is high enough to drive electrons flowing from the conduction band of ZnO to the conductive substrate instead of electrons moving into the electrolyte; this also depends on the redox potential difference between the composite thin films and counter electrode [53, 66-67].

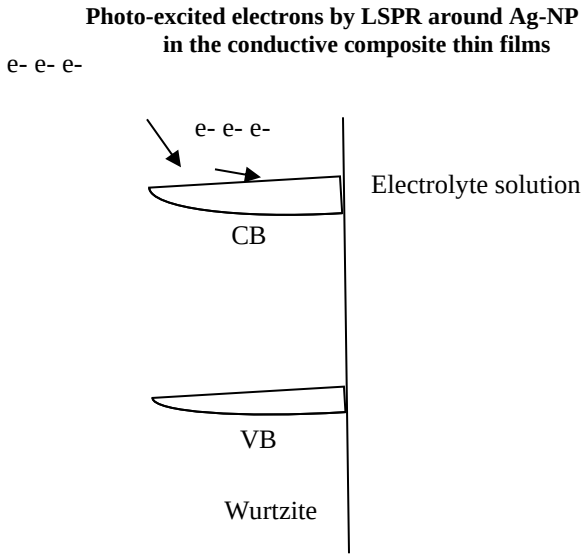

Scheme 2: Proposed mechanism model for cathodic photocurrent generated by Ag-Nanoparticles

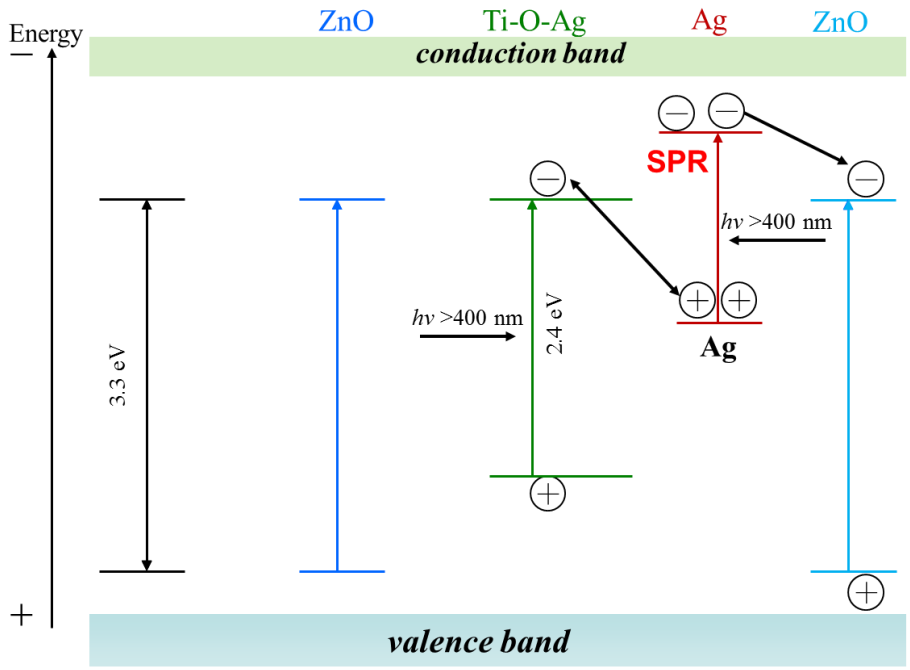

Figure 33: The excitation of electrons in a semi-conductor [30]

Depending on the redox potential difference between the composite thin films and MO, the following [30] primary processes happen when the zinc as a semiconductor is excited in the presence of H_2O and O_2:

$$ZnO \xrightarrow{hv} e^-_{cb} + h^+_{vb}$$

$$h^+_{vb} + H_2O_{(ads)} \rightarrow HO^{\cdot} + H^+$$

$$h^+_{vb} + OH^-_{(ads)} \rightarrow HO^{\cdot}$$

$$e^-_{cb} + O_{2(ads)} \rightarrow O_2^{\cdot -}$$

$$2O_2^{\cdot -} + H_2O \rightarrow 2HO^{\cdot} + 2OH^- + O_2$$

$$\text{-OH + Organic products} \rightarrow \text{Products}$$

Methyl orange is a radical scavenger, therefore both $O_2^{\cdot -}$ and $\cdot OH$ are actively involved in the photo degradation process.

Chapter 5: Conclusions and Recommendations

5.1 Conclusion

Composite thin films of various molar concentrations of silver nanoparticles incorporated into the ZnO matrix were fabricated on quartz glass substrates using the molecular precursor method (MPM). The prepared films were characterized by employing the XRD technique. The XRD patterns showed that the resultant pure silver and pure zinc oxide films contain silver crystallized in the cubic system. The optical band gap was determined and the findings showed that the band gap of ZnO was found by plotting and extrapolating the absorbance vs the photon energy curves. It was also found that the incorporation of silver nanoparticles in the ZnO matrix decreased the optical band gap of ZnO confirming the photocatalytic properties activation of the metal by the noble metal silver. The optical properties of the fabricated composite thin films were studied using UV-Vis spectrometry and it was found that pure ZnO films do not exhibit photo-responsive ability in the visible region. The absorption intensity of ZnO, however, increased considerably at shorter wavelengths, proving that pure ZnO only absorbs in the ultraviolet region. This study also revealed that Ag as noble metal proved to greatly improve the photo response of ZnO in the visible region. The visible light-induced responsiveness of the composite films in this study is specifically attributed to the localized surface plasmon resonance of silver nanoparticles observed at around 410 nm in the wavelength spectrum.

The Ag-NP/ZnO composite thin films were used to study the photocatalytic activity incorporation of Methyl orange dye. The findings were that the composite films greatly improved the photo response of ZnO in the visible region of the UV spectrum. The findings from this study have

proven that silver nanoparticles were influential in enhancing both the UV-Vis response and the photocatalytic activity of composite films under visible light. Therefore, this study consolidates that silver can be deemed as one of the most suitable noble metal dopants for the enhancement of ZnO to be active in the visible region of the wavelength spectrum.

5.2 Recommendations

For the advancement of this work, the film thickness of the thin films can be studied as well as the surface morphology in order to determine the size of the incorporated silver particles.The size of the silver nanoparticles could explain the color of the different films as well as the optical properties. Future researchers can further fill the gap of study by including the electrical properties of the synthesized films as well as studying the photocatalytic properties under UV light irradiation.

6. References

[1] Qu Y, Duan X. Progress, challenge and perspective of heterogeneous photocatalysts. *Chemical Society Reviews*. 2013;42(7):2568-80.

[2] Lee KM, Lai CW, Ngai KS, Juan JC. Recent developments of zinc oxide based photocatalyst in water treatment technology: a review. *Water research*. 2016 Jan 1; 88:428-48.

[3] Srikant V, Clarke DR. On the optical band gap of zinc oxide. *Journal of Applied Physics*. 1998 May 15;83(10):5447-51.

[4] Baruah S, K Pal S, Dutta J. Nanostructured zinc oxide for water treatment. *Nanoscience & Nanotechnology-Asia*. 2012 Dec 1;2(2):90-102.

[5] Truong HB, Huy BT, Ly QV, Lee YI, Hur J. Visible light-activated degradation of natural organic matter (NOM) using zinc-bismuth oxides-graphitic carbon nitride (ZBO-CN) photocatalyst: Mechanistic insights from EEM-PARAFAC. *Chemosphere*. 2019 Jun 1;224:597-606.

[6] Hayashi Y, Takizawa H, Inoue M, Niihara K, Suganuma K. Ecodesigns and applications for noble metal nanoparticles by ultrasound process. *IEEE transactions on electronics packaging manufacturing*. 2005 Oct 24;28(4):338-43.

[7] Altavilla C, Ciliberto E. Inorganic nanoparticles: synthesis, applications, and perspectives. An overview. Inorganic Nanoparticles: Synthesis, Applications, and Perspectives. ed by Altavilla C and Ciliberto E, CRC Press, New York. 2011:1-7.

[8] Zayed M, Ahmed AM, Shaban M. Synthesis and characterization of nanoporous ZnO and Pt/ZnO thin films for dye degradation and water splitting applications. *International Journal of Hydrogen Energy*. 2019 Jun 8.

[9] Aydin C. Synthesis of Pd: ZnO nanofibers and their optical characterization dependent on modified morphological properties. *Journal of Alloys and Compounds*. 2019 Mar 10;777:145-51.

[10] Corro G, Flores JA, Pacheco-Aguirre F, Pal U, Bañuelos F, Torralba R, Olivares-Xometl O. Effect of the Electronic State of Cu, Ag, and Au on Diesel Soot Abatement: Performance of Cu/ZnO, Ag/ZnO, and Au/ZnO Catalysts. *ACS Omega*. 2019 Mar 25;4(3):5795-804.

[11] Sangpour P, Hashemi F, Moshfegh AZ. Photoenhanced degradation of methylene blue on cosputtered M: TiO_2 (M= Au, Ag, Cu) nanocomposite systems: a comparative study. *The Journal of Physical Chemistry C*. 2010 Jul 29;114(33):13955-61.

[12] Vinodkumar R, Navas I, Porsezian K, Ganesan V, Unnikrishnan NV, Pillai VM. Structural, spectroscopic and electrical studies of nanostructured porous ZnO thin films prepared by pulsed laser deposition. *Spectrochimica Acta Part A: Molecular and Biomolecular Spectroscopy*. 2014 Jan 24;118:724-32.

[13] Islam MS, Hossain MF, Razzak SM, Haque MM, Saha DK. Fabrication and characterization of high-crystalline nanoporous ZnO thin films by modified thermal evaporation system. *International Journal of Nanoscience*. 2016 Jun 3;15(03):1640004.

[14] Srinivasarao K, Prameela C, Kala PV, Mukhopadhyay PK. Preparation and characterization of rf magnetron sputtered porous ZnO thin films. *Materials Today: Proceedings*. 2015 Jan 1;2(9):4503-8.

[15] Gür E, Kılıç B, Coşkun C, Tüzemen S, Bayrakçeken F. Nanoporous structures on ZnO thin films. *Superlattices and Microstructures*. 2010 Jan 1;47(1):182-6.

[16] Liu Z, Jin Z, Li W, Qiu J. Preparation of ZnO porous thin films by sol–gel method using PEG template. *Materials Letters*. 2005 Dec 1;59(28):3620-5.

[17] Allah FK, Abé SY, Nunez CM, Khelil A, Cattin L, Morsli M, Bernede JC, Bougrine A, Del Valle MA, Diaz FR. Characterisation of porous doped ZnO thin films deposited by spray pyrolysis technique. *Applied Surface Science*. 2007 Sep 30;253(23):9241-7.

[18] Taka D, Onuma T, Shibukawa T, Nagai H, Yamaguchi T, Jang JS, Sato M, Honda T. Fabrication of Ag dispersed ZnO films by molecular precursor method and application in GaInN blue LED. *physica status solidi* (a). 2017 Mar;214(3):1600598.

[19] Baruah S, K Pal S, Dutta J. Nanostructured zinc oxide for water treatment. *Nanoscience & Nanotechnology-Asia*. 2012 Dec 1;2(2):90-102.

[20] Yan F, Huang L, Zheng J, Huang J, Lin Z, Huang F, Wei M. Effect of surface etching on the efficiency of ZnO-based dye-sensitized solar cells. *Langmuir*. 2010 Jan 29;26(10):7153-6.

[21] Mattox TM, Ye X, Manthiram K, Schuck PJ, Alivisatos AP, Urban JJ. Chemical control of plasmons in metal chalcogenide and metal oxide nanostructures. *Advanced Materials*. 2015 Oct;27(38):5830-7.

[22] Seong S, Park IS, Jung YC, Lee T, Kim SY, Park JS, Ko JH, Ahn J. Synthesis of Ag-ZnO core-shell nanoparticles with enhanced photocatalytic activity through atomic layer deposition. *Materials & Design*. 2019 Sep 5; 177:107831.

[23] Vaiano V, Jaramillo-Paez CA, Matarangolo M, Navío JA, del Carmen Hidalgo M. UV and visible-light driven photocatalytic removal of caffeine using ZnO modified with different noble metals (Pt, Ag and Au). *Materials Research Bulletin*. 2019 Apr 1; 112:251-60.

[24] Schuyten S, Guerrero S, Miller JT, Shibata T, Wolf EE. Characterization and oxidation states of Cu and Pd in Pd–CuO/ZnO/ZrO2 catalysts for hydrogen production by methanol partial oxidation. *Applied Catalysis A: General*. 2009 Jan 15;352(1-2):133-44.

[25] Daniel L, Nagai H, Yoshida N, Sato M. Photocatalytic activity of vis-responsive Ag-nanoparticles/TiO2 composite thin films fabricated by molecular precursor method (MPM). *Catalysts*. 2013 Sep;3(3):625-45.

[26] Daniel LS, Nagai H, Sato M. Absorption spectra and photocurrent densities of Ag nanoparticle/TiO_2 composite thin films with various amounts of Ag. *Journal of materials science*. 2013 Oct 1;48(20):7162-70.

[27] Sangpour P, Hashemi F, Moshfegh AZ. Photoenhanced degradation of methylene blue on cosputtered M: TiO_2 (M= Au, Ag, Cu) nanocomposite systems: a comparative study. *The Journal of Physical Chemistry C*. 2010 Jul 29;114(33):13955-61.

Dweydari AW, Mee CH. Work function measurements on (100) and (110) surfaces of silver. *Physica status solidi (a)*. 1975 Jan 16;27(1):223-30.

[28] Nagai H, Sato M. Heat treatment in molecular precursor method for fabricating metal oxide thin films. Heat Treatment—Conventional and Novel Applications; Czerwinski, F., Ed. 2012 Sep 26:297-322.

[29] Royal Society of Chemistry. Composite materials. Weblog. Available from: http://www.rsc.org/Education/Teachers/Resources/Inspirational/resources/4.3.1.pdf [Accessed 14th December 2018].

[30] Likius DS. *Electrical Conductivities, Plasmonic Properties and VisResponsive Activities of Ag-Nanoparticles/Titania Composite Thin Films Fabricated Using Molecular Precursor Method (MPM)* (Doctoral dissertation, Kogakuin University (Tokyo, Japan). 2014 Mar.

[31] Upadhyaya M. Composites. History of composite materials. Weblog. Available from: http://shodhganga.inflibnet.ac.in/bitstream/10603/23532/12/12_part-b%20chapter-1.pdf [Accessed 20th December 2018].

[32] Understanding nano. Nanotechnology resources. Nonocomposites, their uses and applications. Weblog. Available from: http://www.understandingnano.com/nanocomposites-applications.htmL [Accessed 20th December 2018].

[33] Daniel LS, Nagai H, Aoyama S, Mochizuki C, Hara H, Baba N, Sato M. Percolation threshold for electrical resistivity of Ag-nanoparticle/titania composite thin films fabricated using molecular precursor method. *Journal of Materials Science*. 2012 Apr 1;47(8):3890-9.

[34] Akram M, Hussain R, Ahmed A, Ahmed A, Awan A, Shahzadi I, et al. Mixed Metal Oxide Composites Synthesis and Energy Storage Related Applications. *Bentham Science Publishers*. 2018;3(1):18-25.

[35] Heo YW, Norton DP, Pearton SJ. Origin of green luminescence in ZnO thin film grown by molecular-beam epitaxy. *Journal of Applied Physics*. 2005 Oct 1;98(7):073502.

[36] Tan ST, Sun XW, Zhang XH, Chen BJ, Chua SJ, Yong A, Dong ZL, Hu X. Zinc oxide quantum dots embedded films by metal organic chemical vapor deposition. *Journal of crystal growth*. 2006 May 1;290(2):518-22.

[37] Horwat D, Mickan M, Chamorro W. New strategies for the synthesis of ZnO and Al-doped ZnO films by reactive magnetron sputtering at room temperature. *physica status solidi (c)*. 2016 Dec;13(10-12):951-7.

[38] Gadallah AS, El-Nahass MM. Structural, optical constants and photoluminescence of ZnO thin films grown by sol-gel spin coating. *Advances in Condensed Matter Physics*. 2013;2013.

[39] Razeen AS, Gadallah AS, El-Nahass MM. Effect of Ag doping on the properties of ZnO thin films for UV stimulated emission. *Physica B: Condensed Matter*. 2018 Jun 1;538:131-7.

[40] Details of the MBE facility at UCL. *Molecular Beam Epitaxy*. Weblog. Available from: https://www.ee.ucl.ac.uk/about/MBE [Accessed 13th December 2018].

[41] Pan X, Ding P, He H, Huang J, Lu B, Zhang H, Ye Z. Optical properties and structural characteristics of ZnO thin films grown on a-plane sapphire substrates by plasma-assisted molecular beam epitaxy. *Optics Communications*. 2012 Oct 1;285(21-22):4431-4.

[42] k-Space Associates. Metalorganic Chemical Vapor Deposition (MOCVD). Weblog. Available from: https://www.k-space.com/applications/mocvd/ [Accessed 13th December 2018].

[43] Zeng X, Wen X, Sun X, Liao W, Wen Y. Boron-doped zinc oxide thin films grown by metal organic chemical vapor deposition for bifacial a-Si: H/c-Si heterojunction solar cells. *Thin Solid Films*. 2016 Apr 30; 605:257-62.

[44] Deng B, Yan X, Wei Q, Gao W. AFM characterization of nonwoven material functionalized by ZnO sputter coating. *Materials Characterization*. 2007 ;58(10):854-858.

[45] Pathak SS, Khanna AS. Sol–gel nanocoatings for corrosion protection. In Corrosion Protection and Control Using Nanomaterials 2012 Jan 1 (pp. 304-329). *Woodhead Publishing*.

[46] Khan ZR, Khan MS, Zulfequar M, Khan MS. Optical and structural properties of ZnO thin films fabricated by sol-gel method. *Materials Sciences and applications*. 2011 May 5;2(05):340.

[47] Yang S, Zhang Y. Structural, optical and magnetic properties of Mn-doped ZnO thin films prepared by sol–gel method. *Journal of Magnetism and Magnetic Materials*. 2013 May 1; 334:52-8.

[48] Candal R, Martinez-de la Cruz A. Photocatalytic Semiconductors. *Springer International Publishing*. 2015.

[49] Rehman S, Ullah R, Butt AM, Gohar ND. Strategies of making TiO_2 and ZnO visible light active. *Journal of Hazardous Materials*. 2009;(170)560–569.

[50] Li D, Haneda H, Labhsetwar NK, Hishita S, Ohashi N. Visible-light-driven photocatalysis on fluorine-doped TiO_2 powders by the creation of surface oxygen vacancies. *Chemical Physics Letters*. 2005 Jan 11;401(4-6):579-84.

[51] Ullah R, Dutta J. Photocatalytic degradation of organic dyes with manganese-doped ZnO nanoparticles. *Journal of Hazardous materials*. 2008 Aug 15;156(1-3):194-200.

[52] Wang J, Wang Z, Huang B, Ma Y, Liu Y, Qin X, Zhang X, Dai Y. Oxygen vacancy induced band-gap narrowing and enhanced visible light photocatalytic activity of ZnO. *ACS Applied Materials & Interfaces*. 2012 Jul 23;4(8):4024-30.

[53] Tian Y, Tatsuma T. Plasmon-induced photoelectrochemistry at metal nanoparticles supported on nanoporous TiO_2. *Chemical communications*. 2004(16):1810-1.

[54] Speakman SA. Basics of X-Ray Diffraction. Self-User Training for the X-Ray Diffraction SEF. Weblog. Available from: http://prism.mit.edu/xray/introduction%20to%20xrpd%20data%20analysis.pdf [Accessed 21st December 2018].

[55] Raoufi D, Raoufi T. The effect of heat treatment on the physical properties of sol–gel derived ZnO thin films. *Applied Surface Science*. 2009 Mar 15;255(11):5812-7.

[56] Karamaliyev RA, Qajar CO. Optical properties of composite thin films containing silver nanoparticles. Optical properties of composite thin films containing silver nanoparticles. *Journal of Applied Spectroscopy*. 2012;(79)424-429.

[57] Zheng W, Ding R, Yan X, He G. PEG induced tunable morphology and band gap of ZnO. *Materials Letters*. 2017; 201:85-88.

[58] Seo D, Hofmann R. Direct and indirect band gap types in one-dimensional conjugated

or stacked organic materials. *Springer-Verlag*. 1999;102(23-32).

[59] University of Cambridge. Introduction to semiconductors. Direct and indirect bandgap semiconductors. Weblog. Available from: https://www.doitpoms.ac.uk/tlplib/semiconductors/direct.php [Accessed 17th December 2018].

[60] Purica M, Budianu E, Rusu E, Danila M, Gavrila R. Optical and structural investigation of ZnO thin films prepared by chemical vapor deposition (CVD). *Thin Solid Films*. 2002 Feb 1; 403:485-8.

[61] Hong CS, Park HH, Moon J, Park HH. Effect of metal (Al, Ga, and In)-dopants and/or Ag-nanoparticles on the optical and electrical properties of ZnO thin films. *Thin Solid Films*. 2006 Nov 23;515(3):957-60.

[62] Baruah S, K Pal S, Dutta J. Nanostructured zinc oxide for water treatment. *Nanoscience & Nanotechnology-Asia*. 2012 Dec 1;2(2):90-102.

[63] Hosseini SM, Sarsari IA, Kameli P, Salamati H. Effect of Ag doping on structural, optical, and photocatalytic properties of ZnO nanoparticles. *Journal of Alloys and Compounds*. 2015 Aug 15; 640:408-15.

[64] Wang R, Xin JH, Yang Y, Liu H, Xu L, Hu J. The characteristics and photocatalytic activities of silver doped ZnO nanocrystallites. *Applied Surface Science*. 2004 Apr 15;227(1-4):312-7.

[65] Amornpitoksuk P, Suwanboon S, Sangkanu S, Sukhoom A, Muensit N, Baltrusaitis J. Synthesis, characterization, photocatalytic and antibacterial activities of Ag-doped ZnO powders modified with a diblock copolymer. *Powder Technology*. 2012 Mar 1; 219:158-64.

[66] Gupta K, Jana PC, Meikap AK. Optical and electrical transport properties of polyaniline–silver nanocomposite. *Synthetic Metals*. 2010 Jul 1;160(13-14):1566-73.

[67] Wei D, Amaratunga G. Photoelectrochemical cell and its applications in optoelectronics. *Int. J. Electrochem*. Sci. 2007 Oct; 2:897-912.